COMPUTATIONAL INVESTIGATION OF FLAHOVER MECHANISMS USING FIRE DYNAMICS SIMULATOR (FDS)

BY

SANGKYOUNG LEE

THESIS

Submitted in partial fulfillment of the requirements
for the degree of Master of Science in Mechanical Engineering
in the Graduate College of the
University of Illinois at Urbana-Champaign, 2011

Urbana, Illinois

Adviser:

Associate Professor Dimitrios C. Kyritsis

ABSTRACT

A pilot study of the development of flashover in enclosure fires was performed using the Fire Dynamics Simulator (FDS) platform. Practical criteria for flashover commonly proposed in the literature were investigated in the context of FDS modeling to determine similarity between the CFD model, previous experiments and zone-modeling results. The primary focus of the thesis was to determine FDS-generated flashover criteria that are consistent with established guidelines and can be shown to be independent of the specific configuration of the compartment. As such, a parametric study was performed to calculate the time to flashover (TTF) and maximum heat release rate as a function of parameters that relate to compartment height and ventilation configuration.

The computational domain used for this analysis was a 2.4 x 2.4 x 2.4 m^3 cube with a seating chair, table and carpet with a ventilation opening centered in one wall. The results indicated that the FDS-generated flashover criteria of a radiative heat flux of 20kW/m^2 at the floor level and average upper layer temperature of 600℃ were, in most cases appropriate regardless of ceiling height and the configuration of ventilation. However, the results suggest that a ceiling temperature of 600 ℃ is not a good general criterion for flashover. With increasing ceiling height, the TTF increased significantly, even for a series of models that maintained a uniform compartment volume as the ceiling height increased. This latter result suggests that the delay in flashover can be attributed to the change of heat flux from the upper hot gas layer as well as the additional filling volume from a raised ceiling height. Also, modifications in ventilation size and dimension had noticeable effects on the time to flashover and maximum heat release.

ACKNOWLEDGEMENTS

I would like to express my sincere gratitude to Prof. Dimitrios C. Kyritsis whose leadership and dedication has guided me through this project. He has spent countless hours making sure that I am well supported and advised in my work as a student. I would also like to express my appreciation to Dr. Gavin Horn who has patiently advised me even when I was very naïve to this project at the beginning. Thanks also go to my lab mates, David Schmidt, Benjamin Wigg and Farzan Kazemifar for making the lab a little livelier. I am especially grateful for the support and encouragement from my parents, sister, brother, and friends back home.

TABLE OF CONTENTS

LIST OF TABLES

Page

LIST OF FIGURES

Page

CHAPTER 1: Review of the State of the Art

1.1 Background

Fire safety regulation has a major impact on the overall design of a building in many aspects including layout. Rapid development in modern building technology in a few decades significantly increased the complexity of building design. The physical size of buildings increased continuously and the interior design became complex, which introduces new risk factors in terms of a spread of fire and smoke. The basis of current prescriptive building code and regulations barely provide a necessary guideline to deal with fire hazard in new buildings. As a result, a need of replacing current prescriptive building code with one based on performance has been raised [1]. The problems to be addressed in terms of performance are mainly smoke and heat transport, evacuation of humans, temperature profiles in structure elements, detector or sprinkler activation. The performance of the overall building for a specified design is becoming more important than prescribing which protective treatment is required such as prescribing a number of exits for evacuation purpose. In addition, understanding of enclosure fire phenomena has advanced rapidly, assisted by significant advances in computer technology. As a result of this, the need of computer models that simulate fires in enclosures has increased significantly and appropriate deterministic models are necessary in fire safety engineering. The primary focus of this thesis is on the phenomenon of flashover, because flashover has a strong relation with these issues.

1.2 Flashover

Figure 1.1 shows the five stages of development of a typical compartment fire, namely: ignition, growth, flashover, fully developed and decay [2]. Flashover is the transition from

growth to the fully developed stage, as indicated in Fig. 1.1. During flashover, all combustible materials in the compartment that are not already on fire simultaneously ignite, which is mainly caused by radiation feedback from the hot upper gas layer. Up to this point, heat from the growing fire was partially absorbed by the contents of the room and when the temperature of the contents the compartment reaches its ignition temperature, autoignition occurs. This phenomenon is very significant in fire safety engineering because it signals the end of effective rescue and fire suppression. Also, it occurs rapidly, thus, is extremely dangerous for occupants and fire fighters.

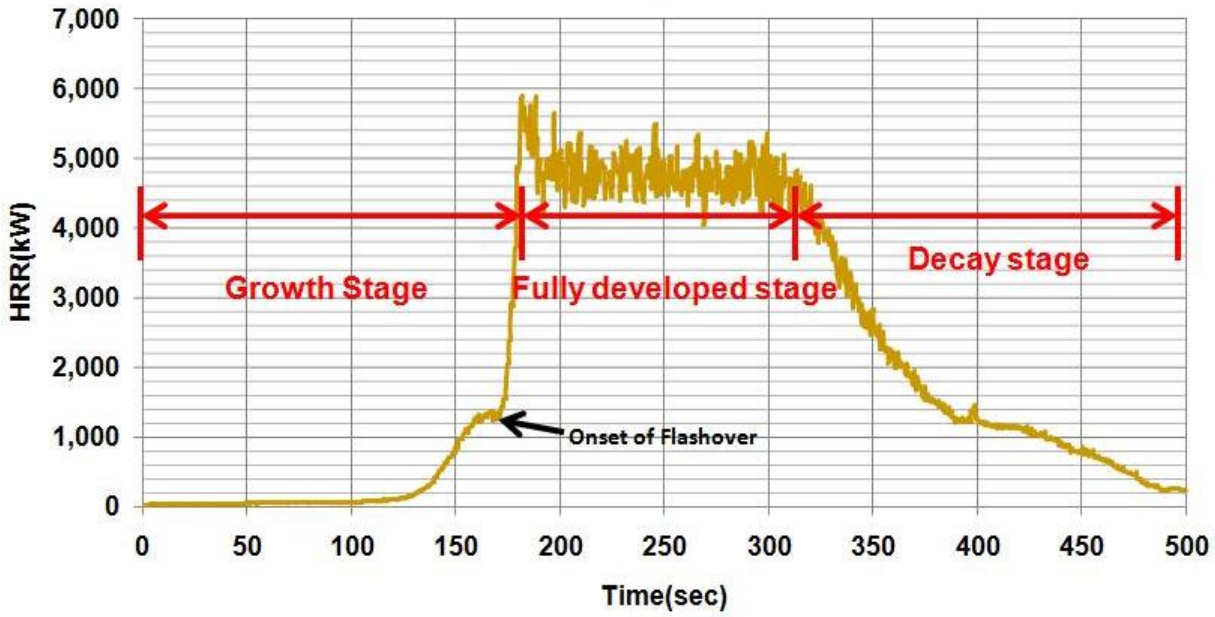

Figure 1.1: General heat release rate profile for a compartment fire

Peacock et al. [3] tabulated the conditions for the onset of flashover observed in several experiments as shown in Table 1.1. There is a range in the numerical values depending on boundary conditions, such as the fuel package and compartment configuration. However, it is reasonable to say that two criteria; a 600℃ upper layer temperature and a 20kW/m^2 heat flux on

the floor level are widely applicable. 600℃ temperature just below the ceiling is also considered by F. M. Liang [4]. Many indicators to describe the occurrence of flashover but only the following four have been validated by experiments:

- 600°C temperature just below the ceiling
- 600°C upper layer temperature
- 20kW/m^2 heat flux to the floor level
- Sudden change in heat release rate

Table 1.1: Conditions at onset of flashover observed by several studies

Source	Temperature(℃)	Heat flux (kW/m^2)
Haggland [5]	600	No data
Fang [6]	450-650	17-33
Budnick and Klein [7-10]	673-771	15
	634-734	No data
Lee and Breese [11]	650	17-30
Babrauskas [12]	600	20
Fang and Breese [13]	706±92	20
Quintirere and McCaffrey [14]	600	17.7-25
Thomas [15]	520	22
Parker and Lee [16]	No data	20

1.3 Fires in Enclosure

1.3.1 Qualitative Description of Enclosure Fires

A fire in an enclosure can develop in multiple ways, mostly depending on the enclosure geometry, ventilation, fuel type and surface area. However, several typical features of development are defined in terms of temperature and mass flow through openings. First of all, with respect to temperature, the development of a typical compartment fire can be divided into five stages, namely: ignition, growth, flashover, fully developed and decay. Since temperature variation in the compartment follows heat release rate, temperature profile variation with time

looks similar to the one of heat release rate profile in the compartment and tracks the onset of flashover well. Observing the mass flow in and out of the enclosure opening is another way of dividing the enclosure fire into typical stages and is represented in Fig. 1.2. P_o and P_i denote pressure outside and inside the compartment, respectively. The pressure profiles are represented by straight lines because the ambient density is assumed to be uniform. Note that higher air density corresponds to a steeper pressure gradient and that hot gas is lighter than cold gas. Once a fuel package ignites, the hot gases in the flame are surrounded by cold gases, thus they rise upward and impinge on the ceiling. Once the plume flow impinges on the ceiling, hot gases spread across the ceiling as a momentum-driven circular jet called a ceiling jet. The ceiling jet eventually reaches the walls of the enclosure and then is forced to move downward along the wall. In the first stage of a fire, the pressure inside is higher than the pressure outside due to the expansion of the upper layer hot gas, as shown in Fig. 1.2 (A). Thus, there is no inflow but only outflow through the opening. If the opening is not at ceiling level, which is typical, in the case of a room fire, the cold gas will be pushed out until the hot gas layer has just reached the top of the opening, and the hot gas will flow out through the opening as shown in Fig. 1.2 (B). In the third stage, the thickness of the ceiling jet increases to the neutral plane height, H_N, where the pressure difference between the inside and outside is zero, so there is no flow at all as shown in Fig. 1.2 (C). Hot gas flows out through the opening above the neutral plane height and fresh air from outside enters through the lower part of the opening. Note that there is an interface which separates the hot and cold gas at H_i, This stage lasts until the room is filled entirely with well-mixed smoke. The last stage, which contains well-mixed smoke, is termed the fully developed fire, indicating that flashover has occurred, as shown in Fig. 1.2 (D).

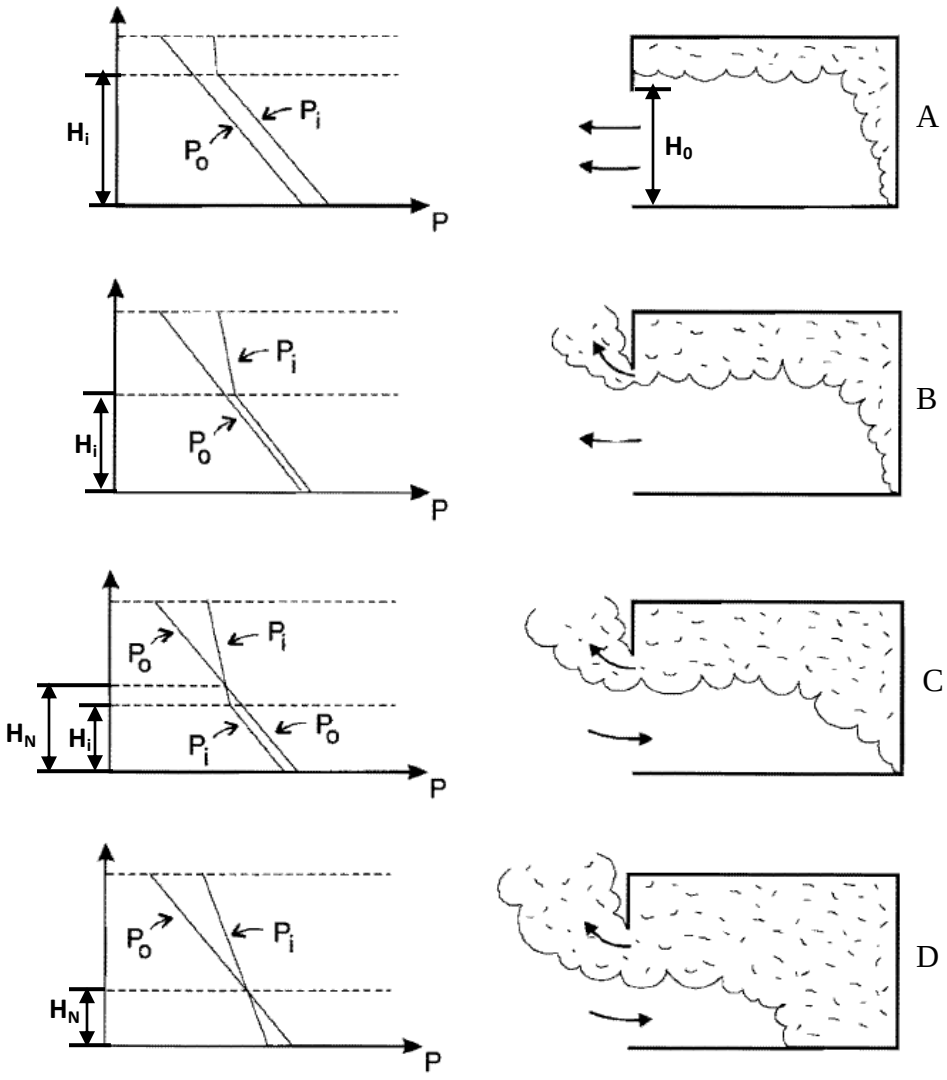

Figure 1.2: The development of pressure profile across the opening [1]

1.3.2 Fire Plumes in Enclosure Fires

In order to study phenomena which are due to the hot gases, the temperature and mass flow rate of the plume flowing upward should be specified. When the mass of hot gases is surrounded by colder gases, the hotter gas will rise upward due to buoyancy. The properties of plumes in compartment fires can be derived with the following assumptions: All of the energy is injected at the point source of origin; there is no radiation heat loss from the plume; the density

inside the plume is uniform, but different than the ambient air (Boussinesq approximation); The speed of horizontal air entrainment at the side edge of the plume, *v* is proportional to the upward plume velocity, *u* along the height, *z*. These assumptions are summarized and presented schematically in Fig. 1.3.

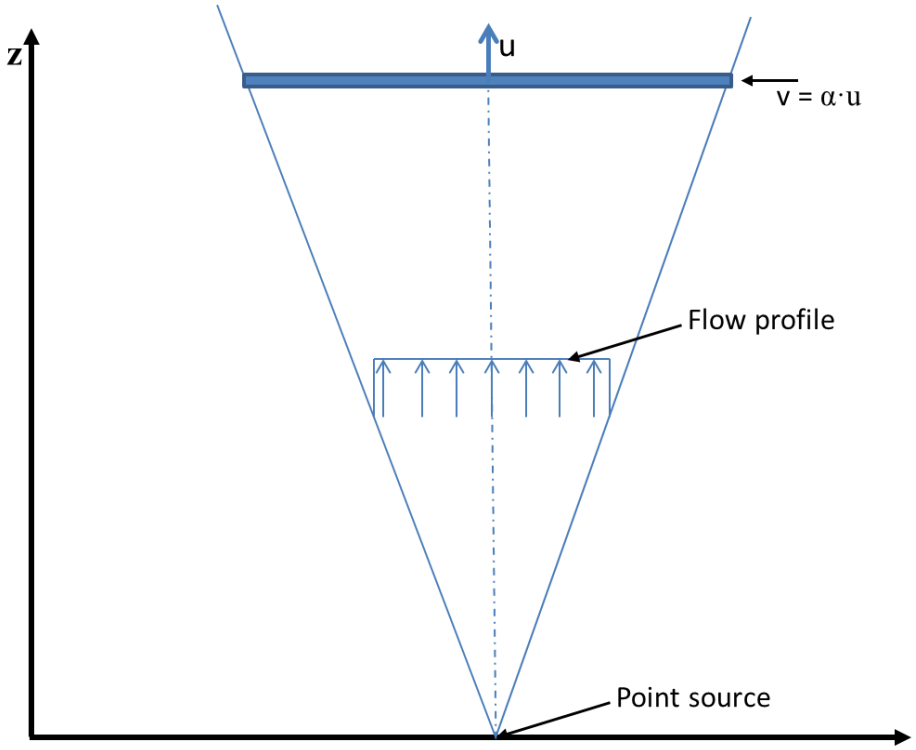

Figure 1.3: The Schematic of Point Source Plume

Practically, the radiative heat release from the plume always takes place in 20% - 40% of total energy release from a fire plume. The Boussinesq approximation only can be applied to the region far above fire source thus the assumptions can be used at heights close to the fire source. However, it has been proven that calculations based on this assumption agree well with experimental data when appropriate adjustment was made. Zukoski [17] carried out experiments where the plume gases were collected in a hood and compiled the results in the correlation:

$$\dot{m}_P = 0.21\left(\frac{\rho_\infty^2 g}{c_p T_\infty}\right)^{1/3} \dot{Q}^{1/3} \cdot z^{5/3} = 0.071\dot{Q}^{1/3} \cdot z^{5/3} \quad (1)$$

where $\dot{m}_P$, ρ_∞, g, c_p, T_∞, $\dot{Q}$ and z denote the mass flow rate of the plume gases, the density of the ambient air, the acceleration of gravity, the specific heat of air, the ambient temperature, the energy released from the fire, and the height of plume captured, respectively. The temperature difference between the hot and cold gases was calculated using $\dot{Q} = \dot{m}_p c_p \Delta T$. Equation (1) showed reasonable agreement with the experimental values but the mass flow rate was under-estimated somewhat due to the unrealistic assumptions. Thus Heskestad [18] improved the point source assumption by introducing a "virtual origin". He also introduced the convective energy release rate, Q_c instead of the total heat release rate, Q and dropped the Boussinesq approximation in the calculations so as to avoid under-estimation. As a result, his plume equation contained a z-z_0 term, the height difference between the virtual origin and the actual burner, instead of only a z term with an extra energy release term.

$$\dot{m}_P = 0.071 \cdot {\dot{Q}_c}^{1/3}(z - z_0)^{5/3} + 0.00192 \cdot \dot{Q}_c \quad (2)$$

McCaffrey [19] performed experiments and obtained the plume mass flow rate relationship:

$$\dot{m}_P \propto {\dot{Q}_c}^{1/3} z^{5/3} \quad (3)$$

Note that the exponential constants for the heat release rate and the height are the same for the three expressions introduced. It is well-established that the plume mass flow rate depends on the heat release rate from the fuel source and the height of the plume captured.

1.3.3 Ventilation-Controlled Enclosure Fires

When the fire grows toward flashover and there is not enough oxygen available to combust most of the pyrolyzing fuel in the compartment, the fire becomes ventilation-controlled.

The energy release rate of the fire is determined by the amount of oxygen that enters the openings, thus this fire is termed ventilation-controlled. Fires in compartments with windows are mostly assumed to be ventilation-controlled, thus, the onset of flashover in a typical single room is affected by the ventilation conditions. The temperature and the mass flow rate of gases in compartment fires are key parameters to predict the onset of flashover and the heat released. McCaffrey et al. [20] used energy conservation and correlations from his experimental data and derived expressions for the upper layer temperature, T_u, the mass flow rate of hot gas out of openings, $\dot{m}_h$ and the mass flow rate of cold air in through openings, $\dot{m}_a$, in a compartment, as

$$\Delta \mathrm{T} = \mathrm{T}_u - \mathrm{T}_\infty = 480 \left(\frac{\dot{Q}}{\sqrt{g} c_p \rho_\infty T_\infty A_0 \sqrt{H_0}} \right)^{2/3} \left(\frac{h_k A_T}{\sqrt{g} c_p \rho_\infty A_0 \sqrt{H_0}} \right)^{-1/3} \tag{4}$$

$$\dot{m}_h = \frac{2}{3} C_d W_0 H_0^{3/2} \rho_\infty \left[2g \frac{T_\infty}{T_h} \left(1 - \frac{T_\infty}{T_h} \right) \right]^{1/2} \left(1 - \frac{H_N}{H_0} \right)^{3/2} \tag{5}$$

$$\dot{m}_a = \frac{2}{3} C_d W_0 H_0^{3/2} \sqrt{2g} \rho_\infty \sqrt{\frac{(\rho_\infty - \rho_h)/\rho_\infty}{[1+(\rho_\infty/\rho_h)^{1/3}]^3}} \tag{6}$$

where $\dot{Q}$, g , c_p, ρ_∞, ρ_h, T_∞, T_h, A_0, H_0, h_k, A_T, C_d, W_0 and H_N denote the energy release rate of fire, the acceleration of gravity, the specific heat of air, the density of air and hot gas, the temperature of ambient air and hot gas, the area of opening, opening height, effective heat transfer coefficient and total area of the compartment wall of inside, the orifice constriction coefficient, opening width and the height of neutral plane, respectively, as defined in Fig. 1.2. Once the gas temperature is twice the ambient temperature, the density term, $\sqrt{\frac{(\rho_\infty - \rho_h)/\rho_\infty}{[1+(\rho_\infty/\rho_h)^{1/3}]^3}}$ in Eqn. (6), changes very slightly and reaches a maximum of 0.214. And taking the standard values of parameters, the maximum mass flow rate of cold air into an opening was obtained:

$$\dot{m}_{a,max} = 0.5 \cdot A_0 \sqrt{H_0} \tag{7}$$

One of the uses of predicted fire temperature in the compartment is the estimation of the onset of flashover. Babrauskas [21] suggested an expression of the minimum energy release rate required for flashover:

$$Q_{fo,BABRUASKA} = 750A_0\sqrt{H_0} \quad (8)$$

This is a product of the maximum air flow into the compartment and the heat released per mass of air consumed. He experimentally proved that, for most fuels, the heat released per mass of air consumed, $\dot{Q}$ is a constant, approximately 3000kJ/kg and flashover occurs when the total heat release rate from the fire is approximately at $0.4\dot{Q}$. Thomas [22] suggested another expression of the minimum energy release rate required for flashover:

$$Q_{fo,THOMAS} = 378A_0\sqrt{H_0} + 7.8A_w \quad (9)$$

where A_w denotes total area of the compartment-enclosing surface. His expression is intended to improve Babrauskas by including the energy loss from radiation mode to the wall. McCaffrey et al. [20] suggested the minimum energy release rate required for flashover from their experimental data:

$$Q_{fo,McCaffrey} = 620(h_k A_w A_0\sqrt{H_0})^{1/2} \quad (10)$$

where h_k and A_w denote the effective heat transfer coefficient and total area of the compartment-enclosing surface, respectively. Eqn. (8) – (10) contain $A_0\sqrt{H_0}$ in common and it is termed "ventilation factor". Kawagoe [23] found that the rate of burning depended strongly on ventilation factor mainly through experimental work. The onset of flashover is strongly correlated with this term in the ventilation-controlled fires.

1.4 Previous Parametric Studies of Flashover

Kim et al. [24] calculated the development of flashover in a typical single room fire using the zone-modeling, FASTLite and CFAST codes which are both released from National Institute of Standards Technology (NIST). CFAST is a two-zone fire model used to calculate the evolving distribution of smoke, fire gases and temperature throughout compartments of a building during a fire [25]. The FASTLite is a simpler variantion of the CFAST code.

The flashover criteria of Babrauskas [21], Thomas [22] and 600℃ upper layer temperature were used to determine the time to flashover (TTF), and Kim focused on the similarities and differences among the criteria. In Kim's paper, the correlation between the ventilation factor and time to flashover was shown, however, the cause was not well explained. Also, the accuracy of the results was very limited because CFAST could not model fire development according to the geometries and properties of fuel packages. Instead, it used only limited experimental data or a simple curve fit method, the t-square fire model [26]. The T-square fire model simply characterizes the heat release rate of every fire with

$$\dot{Q} = \alpha_f (t - t_0)^2 \tag{11}$$

where α_f, t and t_0 denotes fire growth coefficient, the time length from ignition and the time length of incubation. The fire growth coefficient, α_f determines the rate of fire development and categorizes fires as slow, medium, fast and ultra-fast regardless of the type of fuel, as shown in Table 1.2.

Table 1.2: Values of α for different growth rate [27]

Growth rate	α (kW/s^2)	Time (sec) to reach 1055kW
Ultra-fast	0.19	75
Fast	0.047	150
Medium	0.012	300
Slow	0.003	600

In another paper [28], a number of parameters were evaluated as independent factors affecting on the TTF. The 600℃ upper layer temperature criterion was used in order to determine the time to flashover. The fire growth rate, ventilation opening area, wall material and room area have strong effects and vent height, ceiling height and fire location have minor effects on the time to flashover. However, these results were not explained. This, again, mainly came from the limitations of zone-modeling thus it is pointing to the need for high fidelity modeling in fire engineering.

1.5 Scope of Present Work

In this thesis, the capability of FDS (version 5) to predict flashover in a typical room was evaluated through selected computations. Previous work done with two-zone modeling was limited in terms of sub-model integration and grid resolution. Thus previous parametric studies of flashover were not able to verify the correlations between the indicating parameters and the occurrence of flashover. However, with a significantly enhanced spatial resolution and detailed sub-models, the FDS code can give substantial information, such as the heat release rate at the solid boundaries and the temperatures at any location in the domain, to validate correlations between the parameters and flashover. Computations were not intended to model a specific scenario but rather a typical room fire and focus on the effect of geometric variation. Our primary interest was the time required for flashover to occur. The flashover criteria which are widely accepted in fire-safety engineering were evaluated in terms of their ability to indicate flashover in FDS. Another focus of the thesis was to evaluate flashover criteria that are consistent with established guidelines and are independent of the particular configuration of the compartment. Parametric studies, focusing on the effect of ceiling height and ventilation factor

on flashover were implemented. To further understand the effect of ceiling height on the flashover mechanism, it was varied in two scenarios: constant volume and constant floor area (volume increases linearly with height). The ventilation factor was varied as a function of the total area and aspect ratio. Similar parametric work was conducted with a two zone modeling code which had significant limitations in terms of resolution and fidelity of the sub-models used for various aspects of the physics involved. The results from FDS were compared with those of the zone-modeling code. The capability of FDS for the prediction of stable flame spread was also investigated.

CHAPTER 2: Setup of the Computation and Boundary Conditions

2.1 Computational Fluid Dynamics codes for Fire simulation

2.1.1 Fire Dynamics Simulator (FDS)

In order to investigate the effects of ceiling height and ventilation on estimates of flashover, simulations of compartments with varying dimensions were carried out using Fire Dynamics Simulator (FDS, version 5.5), computational fluid dynamics (CFD) model which was developed by National Institute of Standards and Technology (NIST). The FDS code solves the Navier Stokes equations and is numerically appropriate for low speed flows, with an emphasis on smoke heat transport from fire [29]. FDS performs computations for individual mesh grid in order to describe fire-driven flows using a number of sub-models. Smokeview is a scientific visualization program that was developed in order to present the results of FDS computations.

2.1.1.1 Conservation Equations

Ideal gas law and conservation of mass, momentum, energy and species are solved simultaneously using FDS. FDS uses the low-Mach number approximation. This low-Mach number assumption filters out the effects of acoustic waves while allowing for large variations in temperature and density. The low-Mach number assumption serves two purposes: it allows for the time step in the numerical algorithm to be bounded by the flow speed, not sound speed. Also, the number of dependent variables can be reduced by making the pressure term as only a function of position in the energy conservation equation. For turbulence modeling, both Large Eddy Simulation (LES) and Direct Numerical Simulation (DNS) are used in FDS. LES models the dissipative process in order to determine physical properties of substances, which occurs on a

smaller scale than the numerical grid, while, in DNS, physical properties such as conductivity and viscosity can be used directly. Most FDS calculations are performed with LES, because DNS requires a small numerical grid on the order of 1mm or less, which involves huge computational cost.

2.1.1.2 Combustion Model

In FDS, gaseous combustion is described in two ways, using a mixture fraction model and a finite-rate approach. When the finite rate approach is used, FDS requires a large amount of computational time because it tracks each process individually. Thus, the chemical reaction is assumed to be infinitely fast so all parameters related to finite-rate chemical kinetics are excluded from the analysis. Using an infinite rate reaction sheet approximation, the problem of non-premixed combustion is solved with the use of the mixture fraction.

The mixture fraction, Z can be expressed as a linear combination of the fuel and oxygen mass fractions:

$$\mathrm{Z} = \frac{sY_F - (Y_{O_2} - Y_{O_2}^{\infty})}{sY_F^1 + Y_{O_2}^{\infty}} \tag{12}$$

where s is the stoichiometric ratio of fuel and oxygen, Y_F and Y_{O_2} are the mass fraction of fuel and oxygen, respectively, Y_F^I is the fuel mass fraction in the fuel stream and ∞ denotes the ambient condition. Eqn. (12) is valid in well-ventilated fires which assume instantaneous reaction of fuel and oxygen which are separated by the flame sheet. Z can be shown to be equal to :

$$\mathrm{Z} = \frac{1}{Y_F^I}\left(Y_F + \frac{W_F}{xW_{CO_2}}Y_{CO_2} + \frac{W_F}{xW_{CO}}Y_{CO} + \frac{W_F}{xW_S}Y_S\right) \tag{13}$$

where Y_F, Y_{CO_2}, Y_{CO} and Y_S are the mass fractions of fuel, carbon dioxide, carbon monoxide and soot, respectively, and x is the number of carbon atoms in the fuel molecule. Soot is included in the expression because soot is assumed to consist of carbon and hydrogen. Equation (13) is a more general form for a compartment fire, because in the under-ventilated fire, fuel and oxygen may co-exist if the shear layer between the fuel and oxidizing stream has a sufficiently large local strain. FDS version 5 uses this generalized form of the mixture fraction.

2.1.1.3 Radiation Model

There are three modes of energy transport modeled in FDS: Conduction, convection and radiation. Convection energy transport is calculated by the solution of basic energy conservation while radiation is included in the divergence of the heat flux vector, $\nabla q''$ in the energy equation. The primary sources of radiation are soot and flame. Soot is assumed to be non-scattering and to have a continuous radiation spectrum, thus it is regarded as a gray medium. The Radiative Transport Equation (RTE) for a non-scattering gas is expressed as:

$$s \cdot \nabla I_\lambda = a[I_b(s) - I_\lambda(s)] \tag{14}$$

where I_λ, s, a, and I_b denotes the radiation intensity at wavelength λ, the direction vector of intensity, the mean absorption coefficient, and the radiation intensity of blackbody, respectively. Incidentally, the mean absorption coefficient, a, is pre-calculated in FDS by employing RADCAL. And the intensity term is

$$I_b(s) = \sigma T(s)^4 \tag{15}$$

where σ and T(s) denote the Stefan-Boltzman constant and temperature, respectively. As seen in the equation, radiative heat flux is proportional to T^4, so a very accurate temperature calculation is necessary. It is challenging to compute temperature accurately in the flame due to limited

spatial resolution. The temperatures in the flame are under-estimated if the resolution is not fine enough to resolve the flame since the flame sheet occupies only a small part of the grid. Thus, in order to resolve this limitation, FDS chooses the larger intensity value between the one calculated from the empirical radiation loss term, $\chi_r \dot{q}'''$ from the NIST database, and from the estimated temperature in the flame as shown in Eqn. (16). For the outside of flame, it is believed that the estimation of the temperature is reliable, thus FDS uses the intensity from this estimate as shown in Eqn. (17):

$$\mathrm{a} \cdot \mathrm{I}_b = \max\left(\frac{\chi_r \dot{q}'''}{4\pi}, \frac{a \cdot \sigma T^4}{\pi}\right) \qquad inside\ the\ flame \tag{16}$$

$$= \frac{a \cdot \sigma T^4}{\pi} \qquad outside\ the\ flame \tag{17}$$

where χ_r is an empirical estimate of the local fraction of the energy emitted as thermal radiation and $\dot{q}'''$ is the chemical heat release rate per unit volume.

2.1.1.4 Pyrolysis Model

With specified heat release rate, FDS adjusts the mass consumed on the surface of solid fuel packages according to following expression.

$$\dot{\mathrm{m}}''_f = \frac{f(t)\dot{q}''_{SPECIFIED}}{\nabla H} \tag{18}$$

where $f(t)$, $\dot{q}''_{SPECIFIED}$ and ∇H denote the time ramp, specified heat release rate per unit area, and the gradient of total enthalpy at the surface, respectively. FDS assumes that the solid fuel package consists of multiple material layers, and each layer undergoes its pyrolysis process according to the Arrhenius reaction equation:

$$\mathrm{r}_{ij} = A_{ij} Y_i^{n_{ij}} exp\left(-\frac{E_{ij}}{RT}\right) \tag{19}$$

where the subscripts i and j denote i-th material undergoing its j-th reaction and A, Y, n, E, R and T are the pre-exponential factor, the mass fraction of i-th material, order of reaction, activation energy, gas constant and specified temperature of material. However, the parameters of the Arrhenius equation such as the pre-exponential factor and activation energy are not available for realistic materials. Thus, FDS introduces a "reference temperature" for a determination of kinetic constants, A and E. Figure 2.1 illustrates how the reference temperature is determined. Specifically, the reference temperature is defined as the temperature of maximum pyrolysis heat release rate, and therefore mixture fraction decrease, as a function of T. The kinetic constants, E and A for the reaction are now found from:

$$\mathrm{E} = \frac{e r_R}{Y_0} \frac{R T_R}{T} \tag{20}$$

$$\mathrm{A} = \frac{e r_R}{Y_0} e^{E/RT_R} \tag{21}$$

where $r_R, T_R, Y_0,$ R and T denote the reaction rate at the reference temperature, the reference temperature, the mass fraction of substances in the solid, the gas constant and the temperature of the solid.

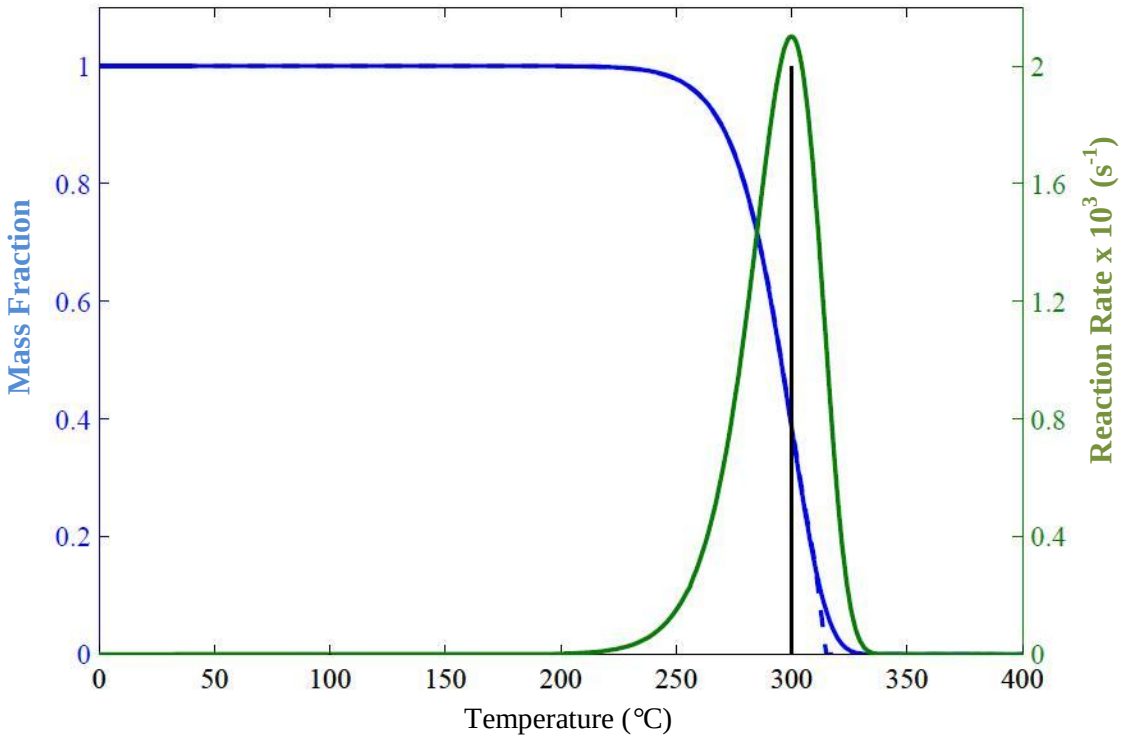

Figure 2.1: Reaction rate and Mass Fraction curve for an arbitrary material with a 300℃ for Reference temperature, Y(0)=1 [29]

2.1.2 CFAST

CFAST is a two-zone fire model which models the system as two distinct compartment gas zones, an upper and a lower volume caused by thermal stratification due to buoyancy, as shown in Fig. 2.2. It solves the mass, energy, momentum conservation equations and involves sub-models for each zone of the plume generated from the fire as a pump of mass from the lower to upper zone. The code input file contains all of the required data, such as prescribed heat release rate, building geometry, material properties and ventilation conditions. CFAST generates an output file in both spreadsheet and Smokeview formats. The spreadsheet includes upper and

lower layer temperature and the wall temperature within each compartment as well as gas species concentration within each layer and the Smokeview visualizes these results.

However, due to its nature, CFAST has some significant limitations. Most limitations are caused by significantly limited grid resolution. Since it has only two stratified zones, flame spread or fire growth on objects cannot be modeled. Also, the straight line interface between upper and lower zone is unrealistic, thus there are restrictions in modeling a fire that generates weakly stratified smoke or a large fire that the flame impinging the ceiling. Since fires should be prescribed in order to run CFAST, the scenarios available are very limited. Thus, it was desired to simulate the fires using multi-dimensional modeling such as FDS, which provides increased simulation capabilities.

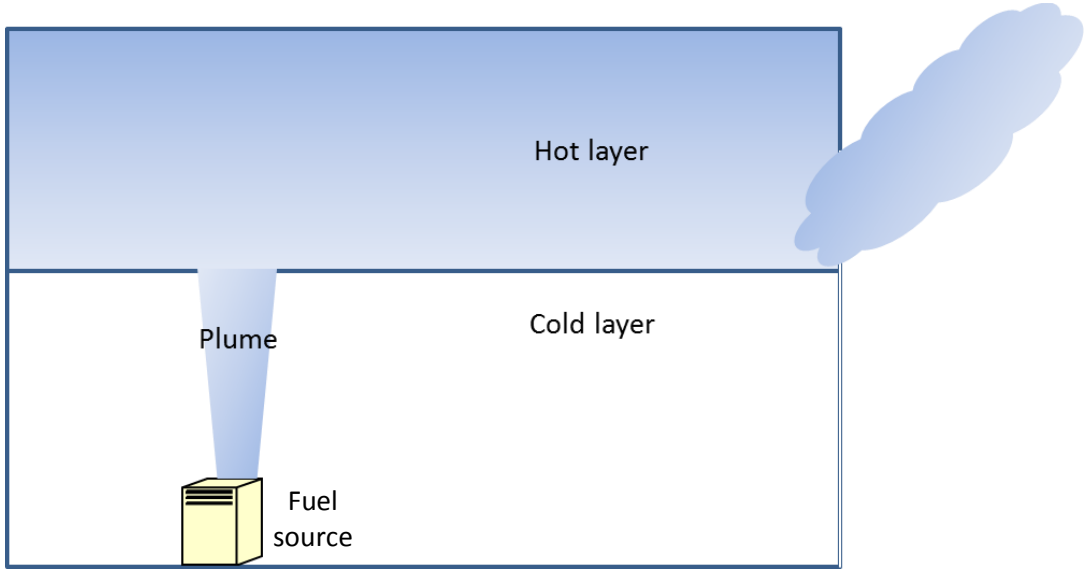

Figure 2.2: Two-Zone modeling of a Fire in an Enclosure

2.2 Computational setup for FDS

2.2.1 Geometry

A computational domain was generated in order to perform parametric studies. The compartment measured 2.4m wide x 3.2m deep and 2.4 m high, but height was adjusted to investigate the ceiling height effect. The domain was broken down into two regions to account for ambient boundary condition (no boundary, 20℃ and 1 atm). The ambient space was placed outside measuring 2.4m wide x 0.8m deep x 2.4m high and open to the exterior. The geometry is shown on Fig. 2.3. The compartment was enclosed by a thin gypsum wall which was modeled as incombustible. A chair (0.8m x 0.6m x 0.9m) and table (0.6m x 0.7m x 0.8m) were put in each corner and carpet the covered entire floor inside the room. This geometry was held constant in every model to represent a typical scenario of fire growth and spread, so the only difference between simulations is compartment height and ventilation dimensions.

2.2.2 Material Properties and Boundary Conditions

The sensitivity of FDS output to material properties has been established in the FDS-related literature [30, 31] and it is substantial. Setting up the appropriate value of properties is crucial in specific situations, for example, investigating the speed of flame spread and the species produced from the reaction at the surface of solid. However, since we focused on the parametric effect of compartment geometry, the material properties of the carpet, chair and table were simply selected from typical values provided by NIST for common furnishings and materials [32]. Thus, it is necessary to recognize that our computations were not intended to model a specific scenario or furniture but rather a typical room fire and focus on the effect of geometric variation. The wall material was gypsum, which was not assumed to contribute any additional

fuel but allowed heat conduction through the wall. The carpet was set to be combustible, so it acted as fuel source, however, its back side was totally insulated so that there was no heat loss through the floor. The chair had two layers consisting of fabric and foam and the properties were referenced from NIST database. The table was made of wood which consisted of cellulose, water and lignin and pyrolyzed in three steps. Once the wood started pyrolysis, cellulose was converted to 'active', then the active was converted to either combustible gas or the combination of combustible gas and char which functioned as heat sink. Further detailed properties can be found from the source code in the Appendix.

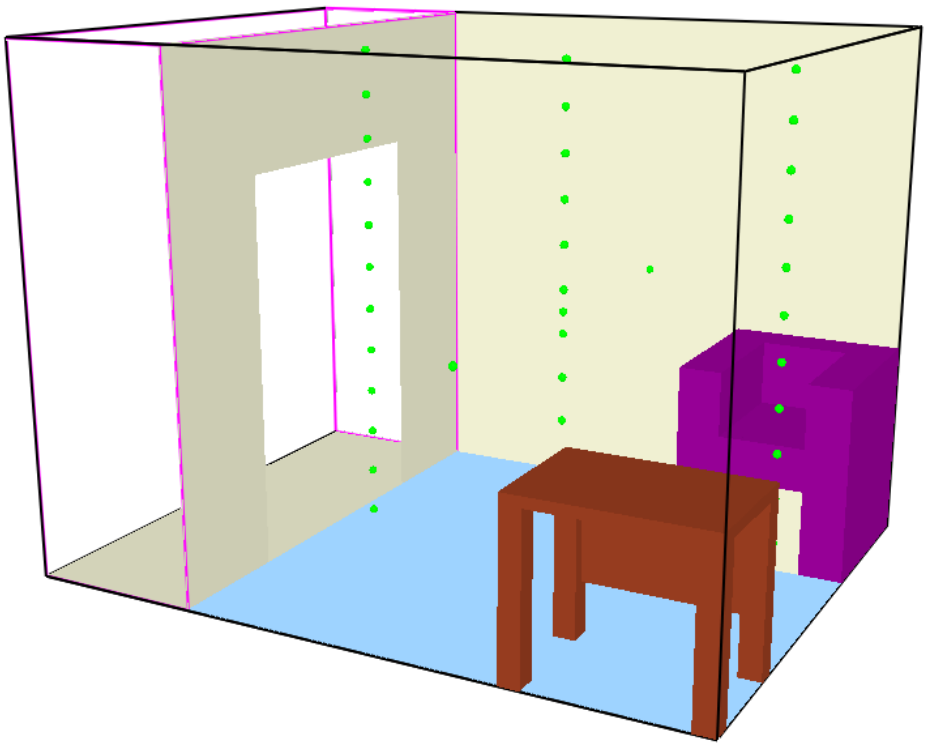

Figure 2.3: FDS simulation domain

A burner which measured 10cm x 10cm was positioned on the chair and the heat release rate per unit area from the burner was set to 3000kW in maximum. It was specified that the heat release rate of burner increased from 0 kW to the maximum in 10 seconds, then stayed constant

140 seconds. At 150 seconds, the burner was turned off so the heat release was only due to the burning of the materials in the compartment. In order to establish temperature criteria for flashover, temperature near the ceiling, floor and ventilation opening was recorded. As seen in Fig. 2.3, three simulated thermocouple trees were positioned in front of the ventilation opening, at the center of the room and near the back wall, and each thermocouple was vertically separated by 20cm, starting at the ceiling.

2.2.3 Grid Resolution

Grid resolution plays important role in FDS calculations as extensive literature has reported [33-36]. Although, in principle, higher resolution produces more accurate computations, this is obviously limited by computational cost, thus it was very important to determine an optimal size of grid resolution. McGrattan [37] suggested 10% of the plume characteristic length, D, as an appropriate length scale and used the following correlations:

$$D = \left(\frac{\dot{Q}}{\rho_\infty c_\infty T_\infty \sqrt{g}}\right)^{2/5} \tag{22}$$

where $\dot{Q}$, ρ_∞, c_∞, T_∞ and g are respectively the total heat release rate (kW), the density at ambient temperature (kg/m3), the specific heat of the gas (kJ/kg·K), the ambient temperature (K), and the acceleration of gravity (m/s^2). Ma [34] suggested that the optimum resolution is 5% of the plume characteristic length. Moreover, he insisted that if the grid size is greater than 5% of the plume characteristic length, FDS tends to under-estimate the flame height and if smaller than 5%, FDS tends to over-estimate the flame height.

Based on these suggestions, a set of computations was implemented in order to investigate grid sensitivity and determine the optimum grid resolution. The test conditions are tabulated in Table 2.1. The 4cm, 5cm, 10cm and 20cm grid size were chosen to perform the grid

sensitivity analysis. The 4cm and 5cm grid size were chosen for the case of less than 5% and 10cm grid size was chosen for the case of 5-10% of the plume characteristic length while 20cm was chosen as larger than the suggested range. 4cm grid size was the minimum size possible to perform with, due to the limit of computational capacity. Theoretically, halving the grid size increases the computation time by a factor of 16. This is because as the number of cells is doubled in each direction, the number of time steps is also doubled because the maximum allowable time step is decreased

Table 2.1: Test Conditions for Grid Resolution Analysis

Test #	Grid Size [m]			Total Cells	D*(5% of D*) [m]
	dx	dy	dz		
1	0.04	0.04	0.04	240000	1.48 (0.074)
2	0.05	0.05	0.05	122880	
3	0.10	0.10	0.10	15360	
4	0.20	0.20	0.20	1920	

Figures 2.4, 2.5 and 2.6 show the comparisons of HRR, temperature at the ceiling level and the upper layer temperature with different grid resolution, respectively. First of all, it is notable that the 20cm grid size failed to calculate the fire. This is because the grid size was too large to perform a computation. Although the 10cm grid size computed the fire, it predicted the onset of flashover much earlier than the two finer grid sizes in terms of HRR, temperature at the ceiling level and the upper layer temperature. Unlike the flame height, the fully developed stage HRR was slightly over-estimated with the coarse resolution. However, finer grid resolution estimated a slightly higher temperature in the fully developed stage but this is not significant for determining time to flashover. It was notable that the shape of the HRR and temperature profiles for the 4cm and 5cm grid size looked similar with an approximately 30 second time difference. Again, since our computations were not intended to model a specific scenario but rather

investigate a general trend of the effects of geometric variation such as ceiling height and ventilation factor, this time delay was acceptable. From this analysis, a 5 cm x 5 cm x 5cm uniform computational grid was selected for calculations.

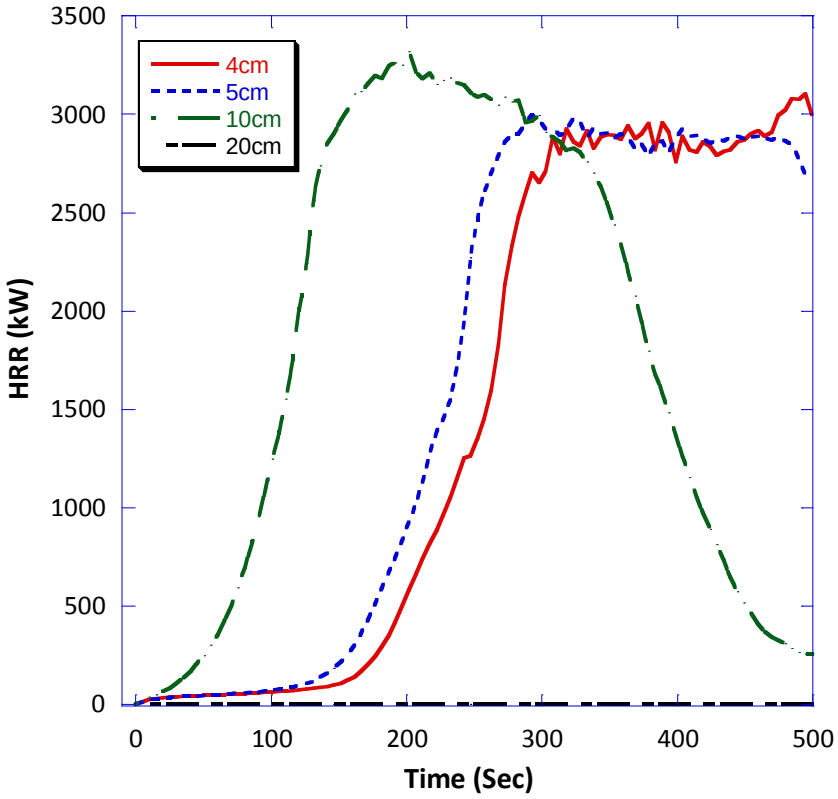

Figure 2.4: Total HRR comparison in Grid Sensitivity Analysis

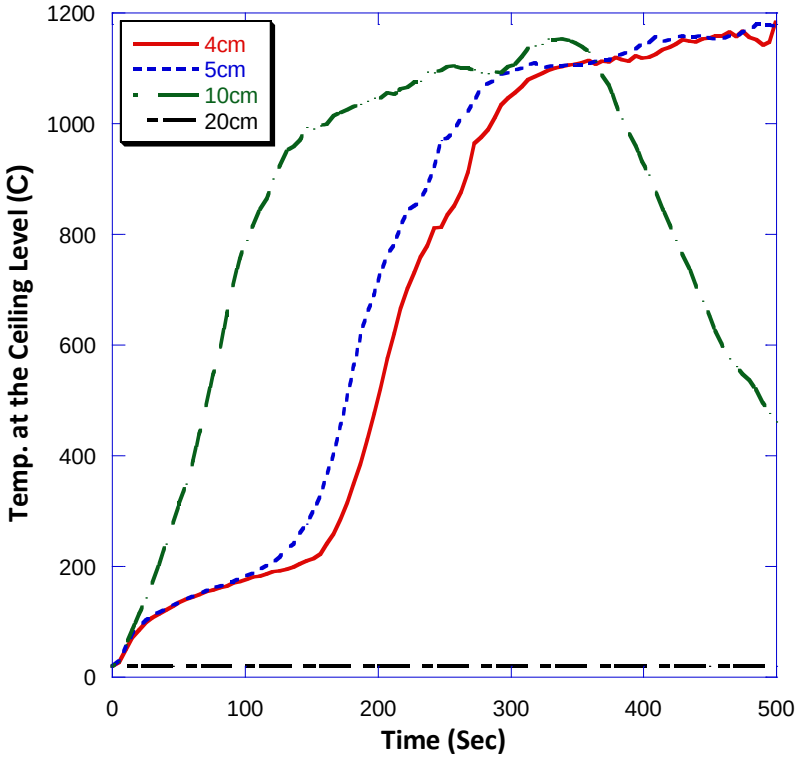

Figure 2.5: Temperature at the Ceiling Level comparison in Grid Sensitivity Analysis

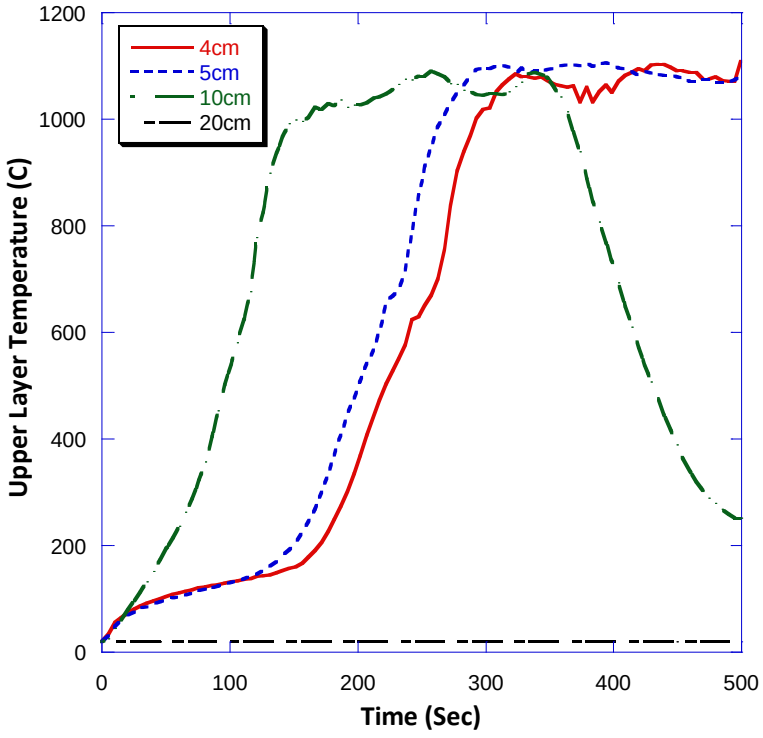

Figure 2.6: Upper Layer Temperature comparison in Grid Sensitivity Analysis

2.2.4 Setup Conditions

Computations were performed in order to evaluate ceiling and ventilation effects on the onset of flashover. The boundary conditions for each simulation are specified in Table 2.2. The effects of ceiling height on flashover were investigated through calculations #1 - #4, by calculating time to flashover, maximum heat release rate, and time duration of maximum heat release after flashover in a compartment with varying ceiling heights and a constant volume. Clearly, increased volume of the compartment is a factor that delays flashover itself, and the effect of ceiling and compartment volume had to be studied independently. The computations were configured so that the change in total area was less than 6% for all cases at constant volume, so that the area available for heat transfer remained practically the same. Models #5 - #7 investigated the effect of increasing volume by changing ceiling height.

In order to investigate the ventilation effects on flashover, six calculations were performed. Four calculations (#8 - #11) were designed to compute the effect of vent shape (aspect ratio) and #12 and #13 were designed to evaluate the effect of the total area of the vent. Wall vents were assumed to be windows that are centered at the centroid of the front wall.

Table 2.2: Initial conditions for calculation

Experiment #		Ventilation Area	Ventilation Dimension (w x l)	Total Volume	Height
Ceiling Height Change	1	$1.44m^2$	1.2m x 1.2m	$11.52m^3$	2.0m
	2				2.4m
	3				2.8m
	4				3.2m
	5			$13.82m^3$	2.4m
	6			$16.13m^3$	2.8m
	7			$18.432m^3$	3.2m
Ventilation Change	8	$1.44m^2$	2.4m x 0.6m	$11.52m^3$	2.4m
	9		1.8m x 0.8m		
	10		0.8m x 1.8m		
	11		0.6m x 2.4m		
	12	$1.00m^2$	1.0m x 1.0m		
	13	$1.96m^2$	1.4m x 1.4m		

CHAPTER 3: Results and Discussion

3.1 Flashover criteria investigation using FDS

As mentioned previously, the criteria for the occurrence of flashover and the time required for flashover to occur are following:

- 600°C temperature just below the ceiling
- 600°C upper layer temperature
- 20kW/m^2 heat flux to the floor level
- Sudden change in heat release rate

It is necessary to recognize that the criteria introduced are not the causes of flashover, instead, they are indicators that signal if and when flashover occurred. Although the criteria signal the onset of flashover, it was very challenging to quantify the time to flashover according to each criterion. Thus, only the quantifiable criteria, 20kW/m heat flux to the floor level, 600℃ temperature of the upper layer and 600℃ temperature at the ceiling level were chosen to evaluate the capability of FDS to indicate the onset of flashover. This work was intended to investigate the reliability of flashover criteria in FDS, and, in a broader sense, the capability of FDS to predict flashover in an enclosure fire.

Time to flashover indicated by heat flux to the floor was determined from the initial moment a 20kW/m^2 heat flux was detected. The FDS output file, Smokeview, is a three-dimensional visualization program which gauges heat flux at the boundary of the room in the time domain. The heat flux gradient at the boundary is indicated by color and varies with time, thus it was easily recognized where and when the target level of heat flux took place as shown in Fig. 3.1. The level of heat flux is indicated with a color bar and the black region between the

table and sofa indicates the location of 20 kW/m^2 heat flux. The time indicator at the bottom shows when this occurred.

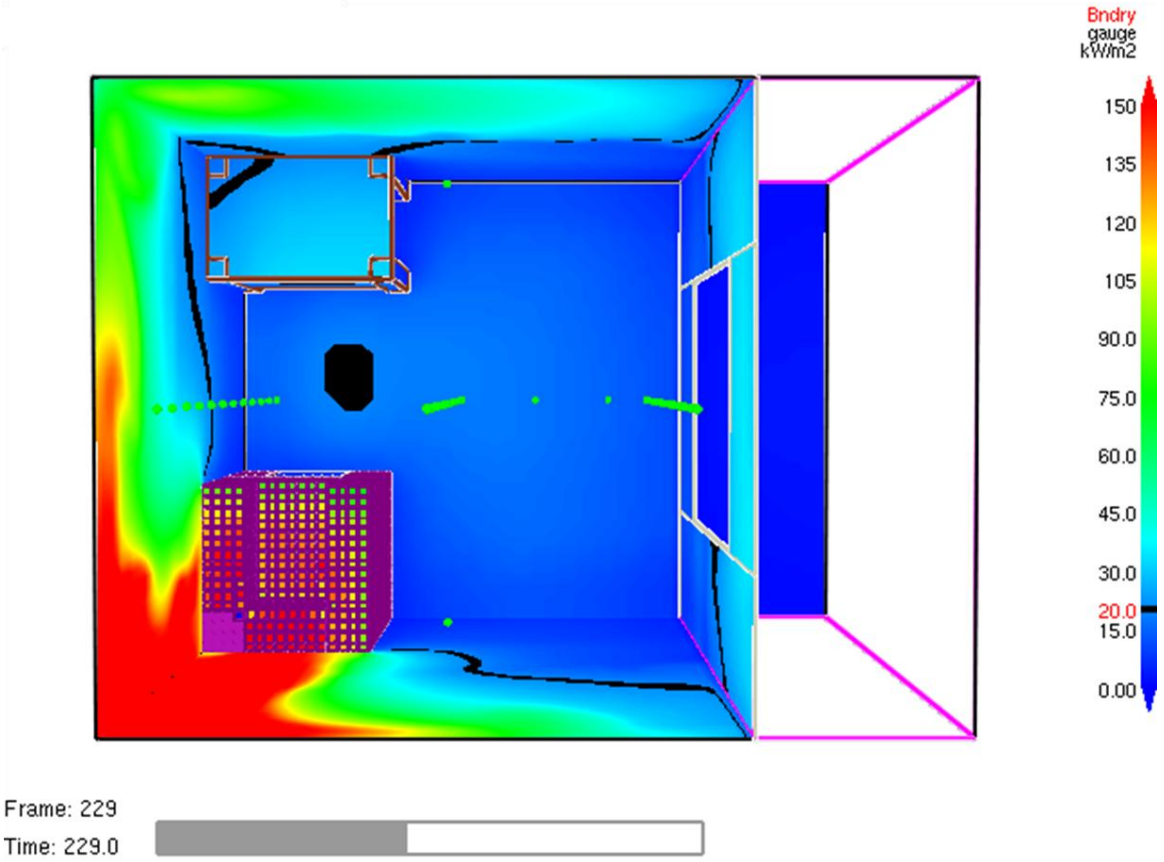

Figure 3.1: Heat flux gradient visualization at the boundary

Time to flashover indicated by upper layer temperature was determined by the initial appearance of the 600℃ temperature. Estimation methods for the gas interface and average temperature of the upper and lower regions in an enclosure fire have been developed, and one such method [38] is used in FDS. Assuming that the vertical profile of temperature is continuous, the upper layer temperature, $T_{u,}$ and the height of the interface, z_{int}, are determined by following equations.

$$(H - z_{int})T_u + z_{int}T_l = \int_0^H T(z)\,dz = I_1 \tag{23}$$

$$(H - z_{int})\frac{1}{T_u} + z_{int}\frac{1}{T_l} = \int_0^H \frac{1}{T(z)}dz = I_2 \quad (24)$$

$$z_{int} = \frac{T_l(I_1 I_2 - H^2)}{I_1 + I_2 T_l^2 - 2T_l H} \quad (25)$$

$$T_u = \frac{\int_{z_{int}}^H T(z)dz}{(H - z_{int})} \quad (26)$$

where T(z), H and T_l denote the continuous temperature profile as a function of height, the ceiling height and the temperature in the lowest mesh cell. The 600℃ temperature at the ceiling level was simply determined by placing thermocouples at the ceiling level. Incidentally, the time step of the output was 0.5 sec, thus, so the measurement error was ±0.5 sec.

The time to flashover indicated by each criterion and the deviations from the time predicted by the HRR criterion are tabulated in Table 3.1. The HRR criterion is defined as a transition between the growth and fully developed stages in the heat release rate. Typically, heat release rate plots generated by FDS are not smooth due to noise. Thus, it was very challenging to determine the moment of transition, so a manual method was implemented, as shown in Fig. 3.2. The other criteria were compared with this HRR criterion. Figure 3.3 shows the correlation between the criteria.

Table 3.1 - The Comparison of TTF Indicated by Introduced Criteria

Exp. #	Time to Flashover (sec)				Deviation from HRR Criterion		
	HRR Criterion	20kW/m^2 Floor Level	600℃ Temp. Upper Layer	600℃ Temp. Ceiling Level	20kW/m^2 Floor Level	600℃ Temp. Upper Layer	600℃ Temp. Ceiling Level
1	210	198	219	182	-5.7	4.3	-13.3
2	240	229	244	193	-4.6	1.7	-19.6
3	265	262	252	192	-1.1	-4.9	-27.5
4	290	292	253	201	0.7	-12.8	-30.7
5	240	229	247	193	-4.6	2.9	-19.6
6	285	282	293	200	-1.1	2.8	-29.8
7	330	328	336	207	-0.6	1.8	-37.3
8	238	222	237	192	-6.7	-0.4	-19.3
9	235	224	241	190	-4.7	2.6	-19.1
10	245	232	254	197	-5.3	3.7	-19.6
11	255	239	266	197	-6.3	4.3	-22.7
12	230	222	234	176	-3.5	1.7	-23.5
13	265	247	268	204	-6.8	1.1	-23.0

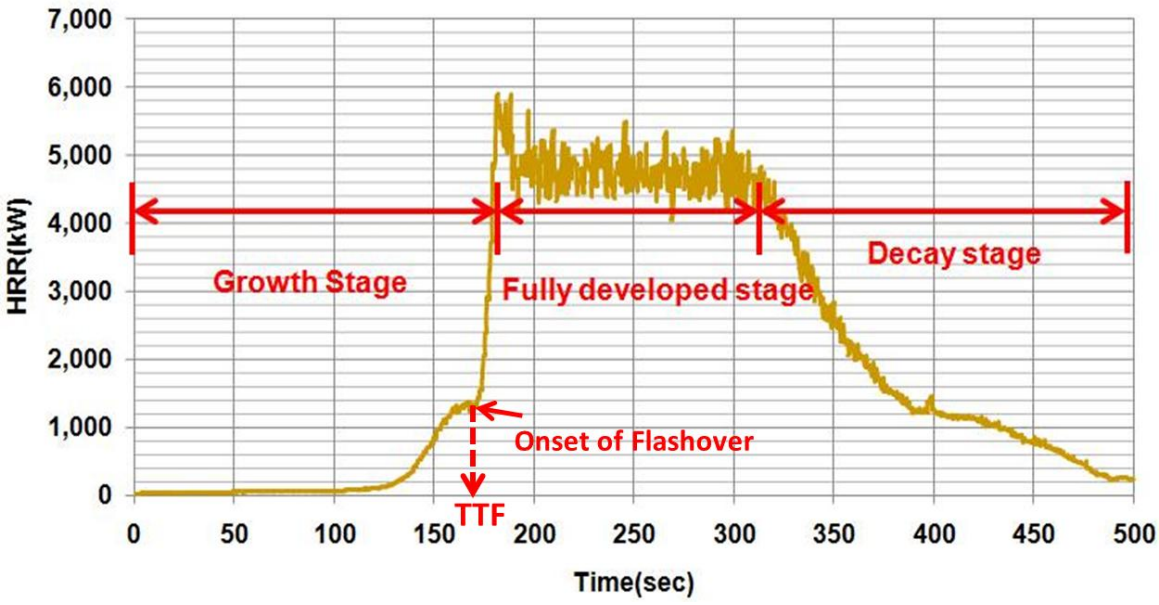

Figure 3.2: TTF determination indicated by HRR criterion

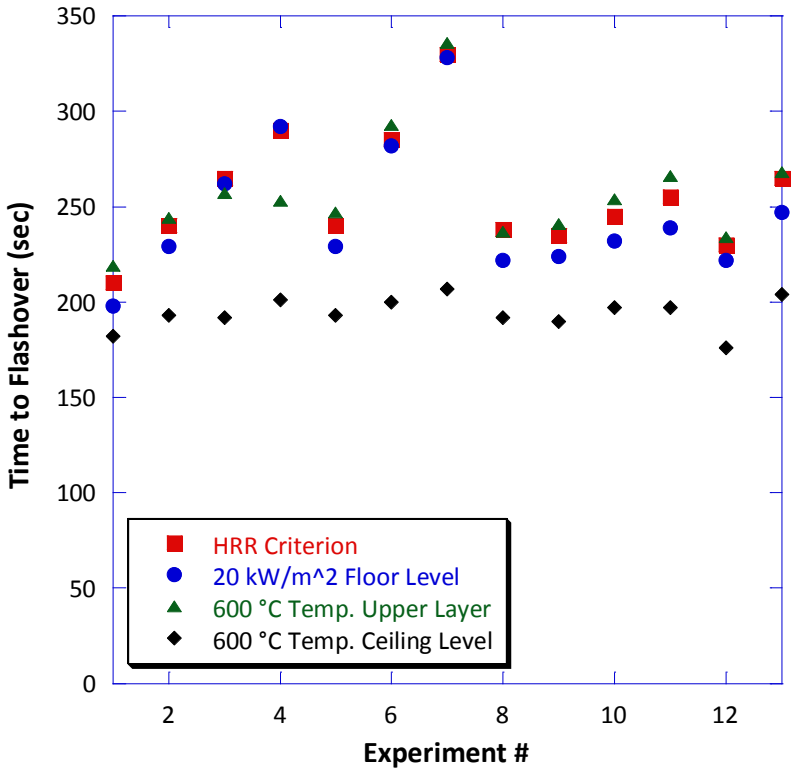

Figure 3.3: TTF comparison indicated by introduced criteria

It was shown that TTF estimated by 20 kW/m^2 heat flux to the floor level and the 600℃ upper layer temperature appeared at nearly the same line independent of the ceiling height, volume, ventilation aspect ratio, and size. These two indicators also showed a strong correlation with the sudden increase in HRR. This implies that in FDS, 20 kW/m^2 radiation flux to the floor level and 600℃ upper layer temperature are reliable indicators of flashover. However, the 600℃ ceiling level temperature criterion underestimated TTF when compared to the others. The deviation was averaged 23.5% and this implies that the 600℃ ceiling level temperature criterion is not a reliable criterion for flashover in FDS without modifications. This high rate of deviation was even worse in higher ceiling height conditions.

The reasoning of these results is because the three indicators are “ordered” with respect to their capability to indicate TTF. As plume gas is pumped to the ceiling, the thickness of the

ceiling jet, filling depth, grows downward. Hot gases are accumulated at the ceiling level, thus, 600℃ temperature at the ceiling level can be easily reached and is the fastest indicator. However, there is a time delay during which the hot gases fill the upper layer of the room, before the average upper layer temperature reaches 600℃. Also, the results showed that 20 kW/m^2 heat flux to the floor occurred slightly earlier than the 600 ℃ upper layer temperature. However, since the deviations between the criteria were not significant (typically less than 6%), it is reasonable to use both criteria for determining TTF in FDS regardless of enclosure geometry and ventilation. The only outlier of earlier prediction of 600℃ upper layer temperature was shown in the highest ceiling height. That is, there was time delay between the 600℃ upper layer temperature and the 20 kW/m^2 heat flux to the floor. This implies the time of heat transfer from hot gas layer to the floor is not negligible in the high ceiling height.

3.2 The Effect of Ceiling Height

The effects of ceiling height variation are shown in Fig. 3.4. As reported in the literature which used two-zone modeling, it was shown that as the height of ceiling increased, the onset of flashover was delayed. When the compartment volume remained constant with increasing ceiling height, the percent increase in TTF for a given percent increase in height was smaller than in the case for which the volume increased proportionally to height.

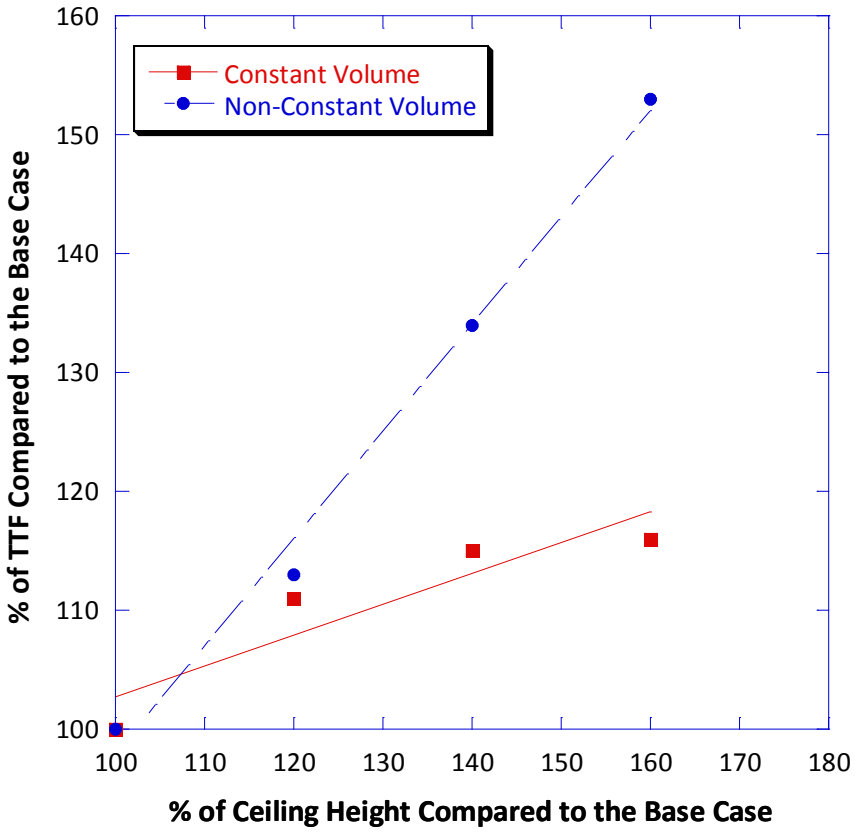

Figure 3.4: TTF vs. Ceiling Height with Non-Constant and Constant Volume

In order to keep uniform volume with the ceiling height, the ceiling area inevitably decreases. On the other hand, when the volume of the compartment is allowed to increase with increasing ceiling height, a larger amount of hot gas needs to build up in the hot upper layer to ultimately cause flashover. That is, it is recognizable that the smaller ceiling area, A_c results in higher filling depth rate, $\dot{h}$, because of following relation:

$$\dot{h} = \frac{\dot{m}}{\rho A_c} \tag{27}$$

where $\dot{m}$ and ρ denote the mass flow rate of gases pumped to the upper layer and the average density of the gas, which do not change with room geometry. Since the amount and kind of fuel package are consistent for a set of computations and the ventilation condition was same, the

plume mass flow rate, $\dot{m}$, should be same here. Higher filling depth rate implies a shorter time for the upper layer gas to reach 600℃. Higher ceiling height which delays TTF, is balanced by the higher filling depth rate, so non-constant volume showed a higher sensitivity of TTF increase to the ceiling height increase.

In order to investigate the computation capabilities of FDS, the results of ceiling height variation are compared with the results of two zone modeling, CFAST and FASTLite [28] in Fig. 3.5. The boundary conditions were the same in three cases but the fuel package was different. Since the boundary conditions were the same, the trends should agree, however, Fig. 3.5 shows that zone modeling underestimates the sensitivity of TTF to volume changes as compared to the FDS computation. It is because the two-zone model has a limit of resolution (two zone) while the field model has a significantly enhanced spatial resolution.

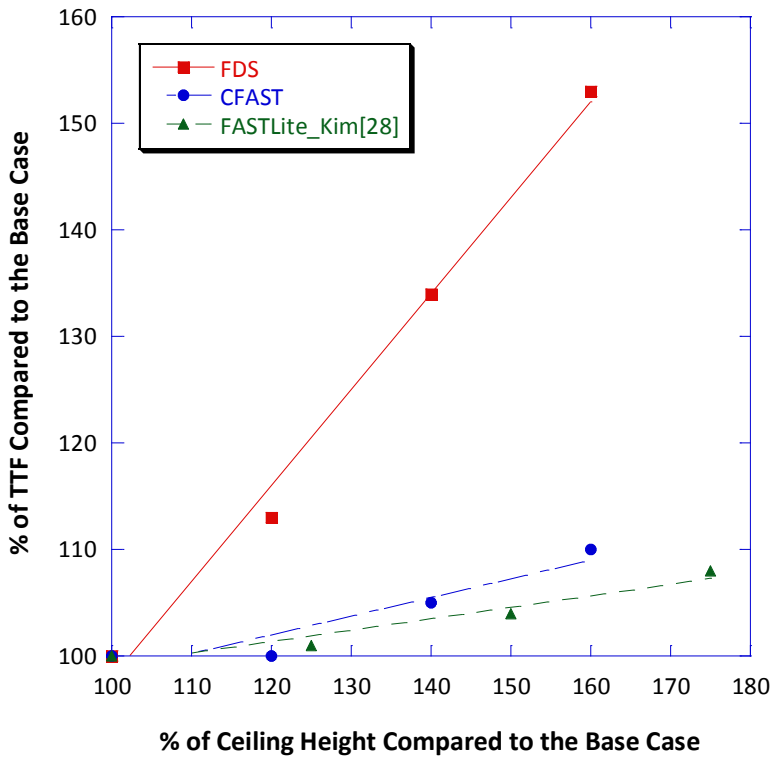

Figure 3.5: Ceiling Height effect comparison between Field modeling and Two-zone modeling

3.3 The Effect of Ventilation Conditions

An additional series of simulations was developed in order to study the dependence of flashover on the ventilation configuration in enclosure fires. All simulations were conducted with a constant 2.4m ceiling height and wall vents were placed with centroid at 1.2m from the floor level. Five calculations (#5, #8 - #11) were intended to compute the effect of vent shape (aspect ratio) and three calculations ((#5, #12, #13) were intended to evaluate the effect of the total area of the vent. Table 3.2 shows the setup conditions with the ventilation factor and the total area of wall inside the compartment. A heat release rate profile generated by FDS is shown in Fig 3.6.

Table 3.2: Setup Conditions for Ventilation Effect Investigation

Variable	Ventilation Dimension	Vent. Area, A_0 [m^2]	Vent. Height, H_0 [m]	Ventilation Factor, $A_0\sqrt{H_0}$	Wall Area, A_w [m^2]
Aspect Ratio	2.4m x 0.6m	1.44	0.6	1.12	33.12
	1.8m x 0.8m		0.8	1.29	
	1.2m x 1.2m		1.2	1.58	
	0.8m x 1.8m		1.8	1.93	
	0.6m x 2.4m		2.4	2.23	
Ventilation Size	1.0m x 1.0m	1.00	1.0	1.00	33.56
	1.2m x 1.2m	1.44	1.2	1.58	33.12
	1.4m x 1.4m	1.96	1.4	2.32	32.60

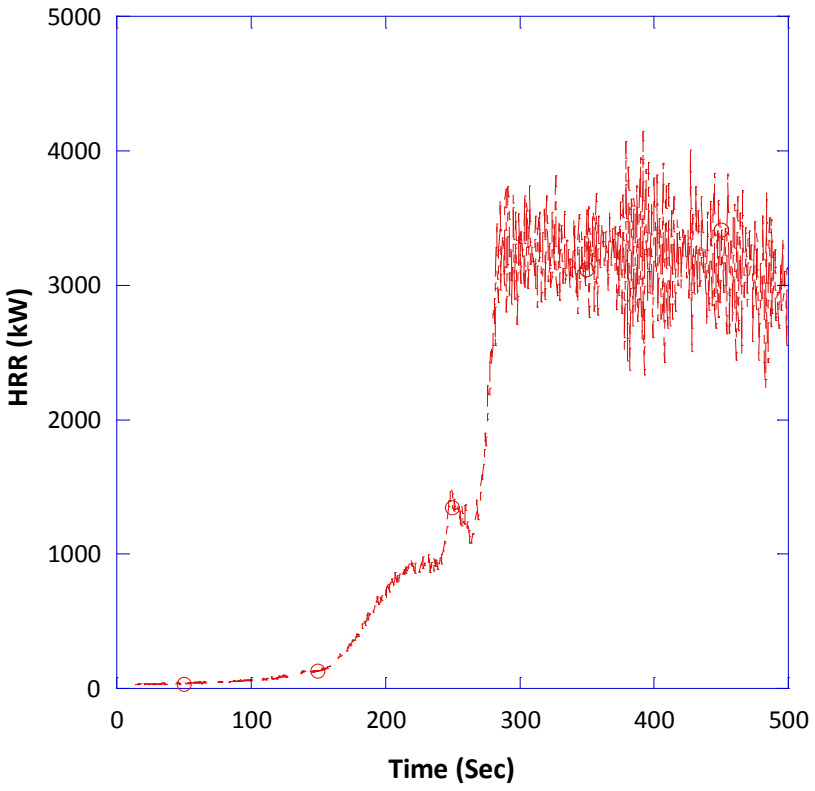

Figure 3.6: Heat Release Rate Profile of 2.4m x 2.4m ventilation, generated by FDS

The heat release rate profile in Fig. 3.6 is similar to one of a typical enclosure fire, however, it is notable that there is a large amount of noise in the fully developed stage. This oscillation appeared in most of the calculations, and this phenomenon iss explained in [39]. The occurrence of flashover results in a good mixing of fresh air entering the room with the combustion products from the fire. This mixing generates vortices, eddies and non-uniform oxygen concentration in the vicinity of the flame sheet. Since the HRR is calculated from the local concentration of oxygen at the flame surface in FDS, the higher HRR appears in an area of higher oxygen concentration while the lower HRR appears in an area of lower oxygen concentration. As a result, fluctuation of the heat release rate profile in the fully-developed stage is caused by this time-varying flame surface. In order to proceed further with analysis of the heat

release rate, a smoothed profile was needed, so a 10-point (5 sec) moving-average method was used. The processed heat release rate profile is shown in Fig. 3.7.

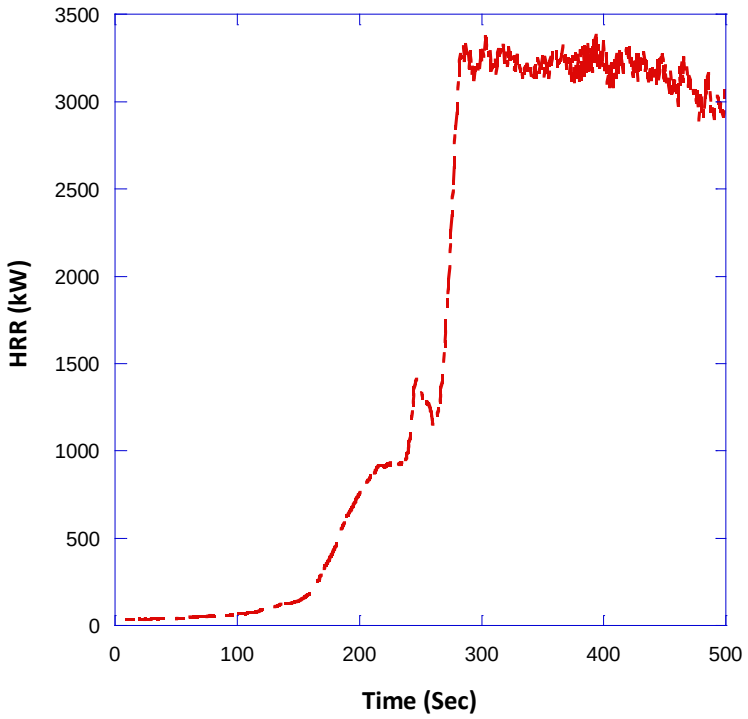

Figure 3.7: A smoothed Heat Release Rate Profile of 2.4m x 2.4m ventilation (10-point moving-average smoothing method applied)

The heat release rate required for flashover and the maximum energy release rate after flashover, which are termed “Pre-Flashover HRR” and “Post-Flashover HRR”, respectively, are tabulated in Table 3.3. The predictions of the pre-flashover HRR from Eqn. (8)-(10), suggested by Babrauskas, Thomas and McCaffrey, respectively, are compared with the ones from FDS calculation. The comparison of pre-flashover and post-flashover HRR with respect to the ventilation factor is illustrated in Fig. 3.8 and Fig. 3.9, respectively.

Figure 3.8 shows that the predictions of the pre-flashover HRR based on previously introduced expressions, Eqn. (8) – (10), have a linear dependence on the ventilation factor;

however, the results from FDS have a constant value independent of the ventilation factor. That is, FDS failed to predict the linear dependence of the minimum energy release rate required for flashover on the ventilation factor. Figure 3.9 shows that the post-flashover HRR is linearly dependent on the ventilation factor. The linear behavior of the maximum energy release rate in the fully developed stage is well supported by the theory [20], and, FDS was able to predict it.

Table 3.3: A comparison of Pre-Flashover and Post-Flashover HRR

	Ventilation Dimension	$A_0\sqrt{H_0}$	Pre-Flashover HRR (kW)				Post- Flashover HRR (kW)
			FDS	Babrauskas[21]	Thomas[22]	McCaffrey[20]	
Vent. Shape	2.4m x 0.6m	1.12	966	840	682	827	2407
	1.8m x 0.8m	1.29	912	968	746	888	3038
	1.2m x 1.2m	1.58	914	1185	856	983	3387
	0.8m x 1.8m	1.93	912	1448	988	1086	3937
	0.6m x 2.4m	2.23	961	1673	1101	1167	4196
Vent. Size	1.0m x 1.0m	1.00	916	750	640	787	2427
	1.2m x 1.2m	1.58	914	1185	856	983	3387
	1.4m x 1.4m	2.32	960	1740	1131	1181	4697

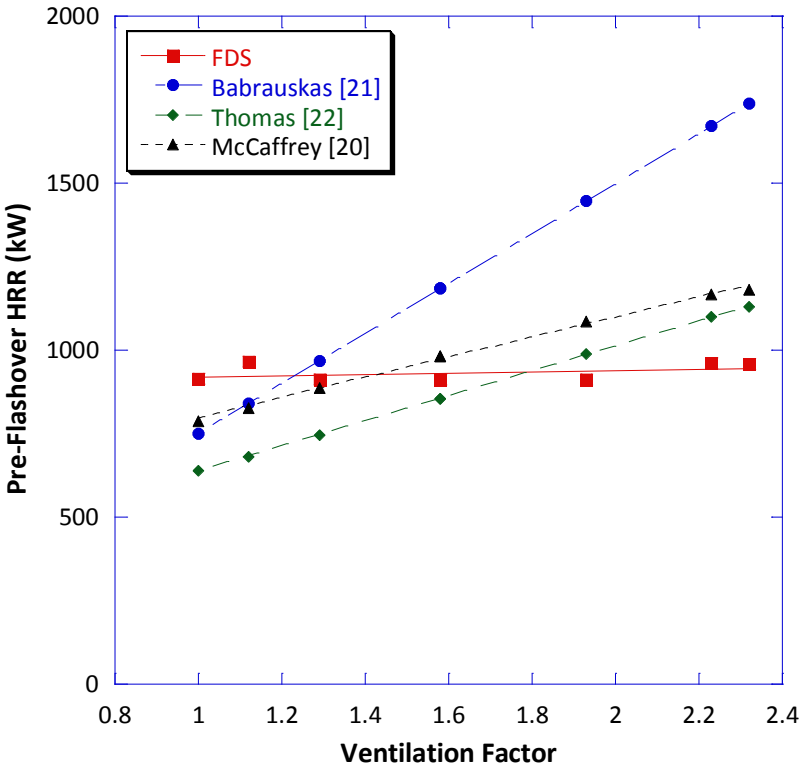

Figure 3.8: Pre-Flashover vs. Ventilation Factor

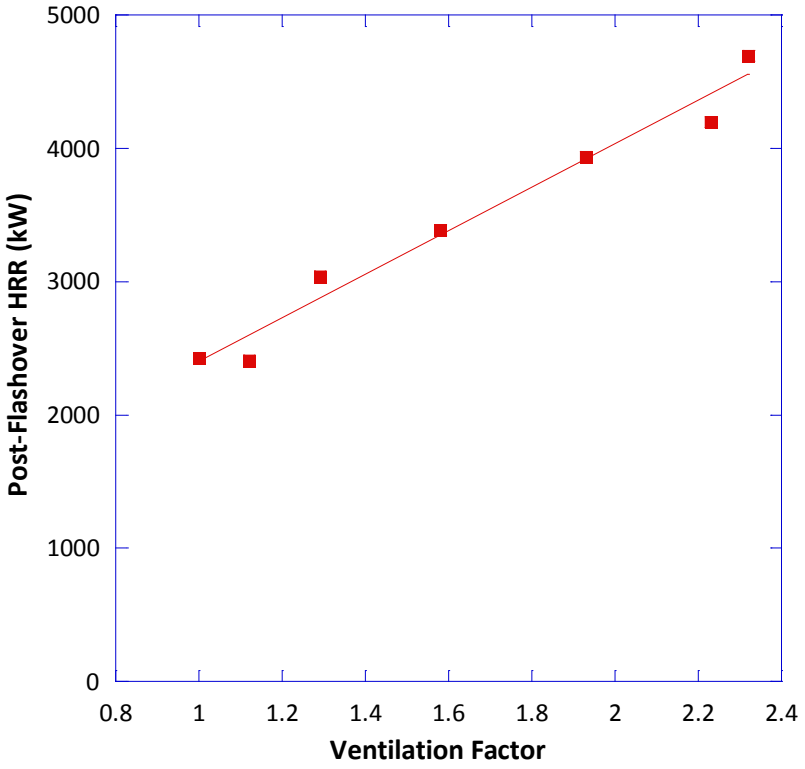

Figure 3.9: Post-Flashover vs. Ventilation Factor

The dependence of TTF on ventilation conditions is tabulated in Table. 3.4 and the relations of the ventilation height, ventilation size and ventilation factor versus TTF are illustrated in Fig. 3.10 -3.12, respectively. Overall, CFAST slightly underestimated TTF when the ventilation condition varied, however, unlike in the case of varying ceiling heights, the sensitivities were similar with those in FDS. Figures 3.10-3.12 show the linear dependence of TTF on the ventilation height and size, as well as ventilation factor. FDS accurately predicts increasing ventilation factor, ventilation height, and ventilation size delay the occurrence for flashover. In ventilation configurations which have higher ventilation factors, the air can more easily flow into and out of the compartment. The additional inflow increases the post flashover heat release rate, and improves hot gas outflow, delaying TTF.

Table 3.4: TTF vs. Ventilation Conditions

	Ventilation Dimension	Vent. Area, A_0 [m^2]	Vent. Height, H_0 [m]	Ventilation Factor, $A_0\sqrt{H_0}$	TTF [Sec]	
					FDS	CFAST
Ventilation Shape	2.4m x 0.6m	1.44	0.6	1.12	237	200
	1.8m x 0.8m		0.8	1.29	241	210
	1.2m x 1.2m		1.2	1.58	247	210
	0.8m x 1.8m		1.8	1.93	254	220
	0.6m x 2.4m		2.4	2.23	266	230
Ventilation Size	1.0m x 1.0m	1.00	1.0	1.00	234	190
	1.2m x 1.2m	1.44	1.2	1.58	247	210
	1.4m x 1.4m	1.96	1.4	2.32	268	240

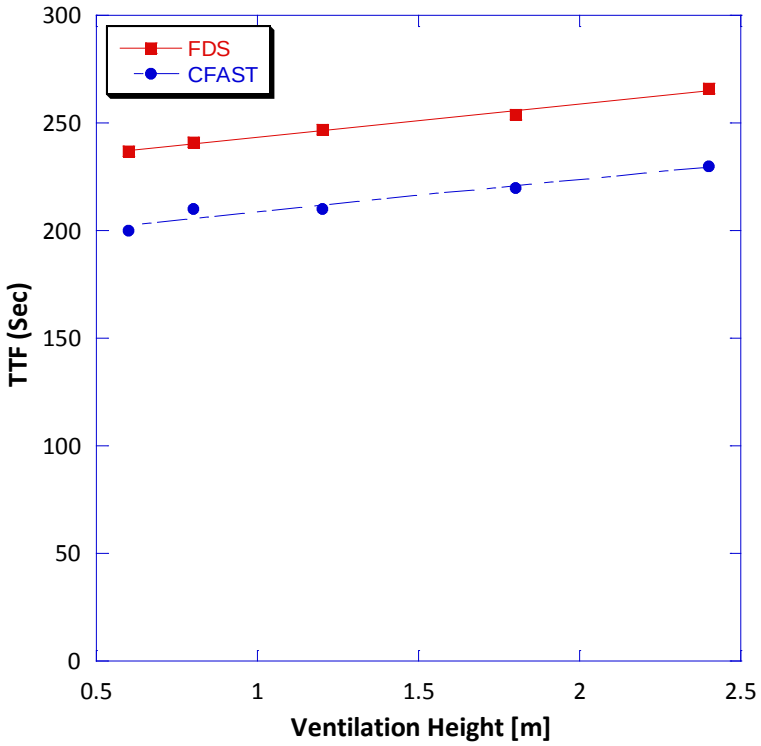

Figure 3.10: TTF Prediction of FDS and CFAST depending on Ventilation Height

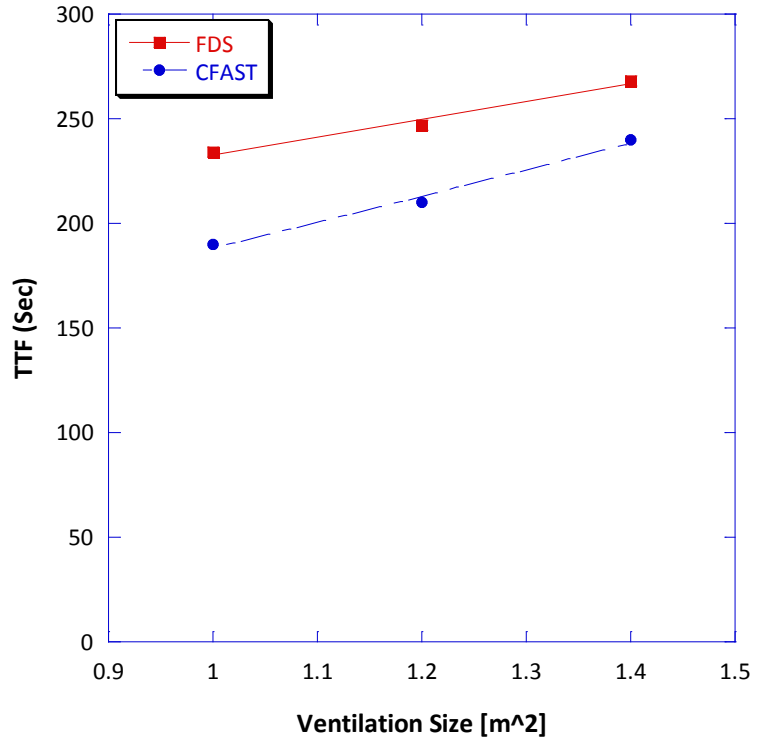

Figure 3.11: TTF Prediction of FDS and CFAST depending on Ventilation Size

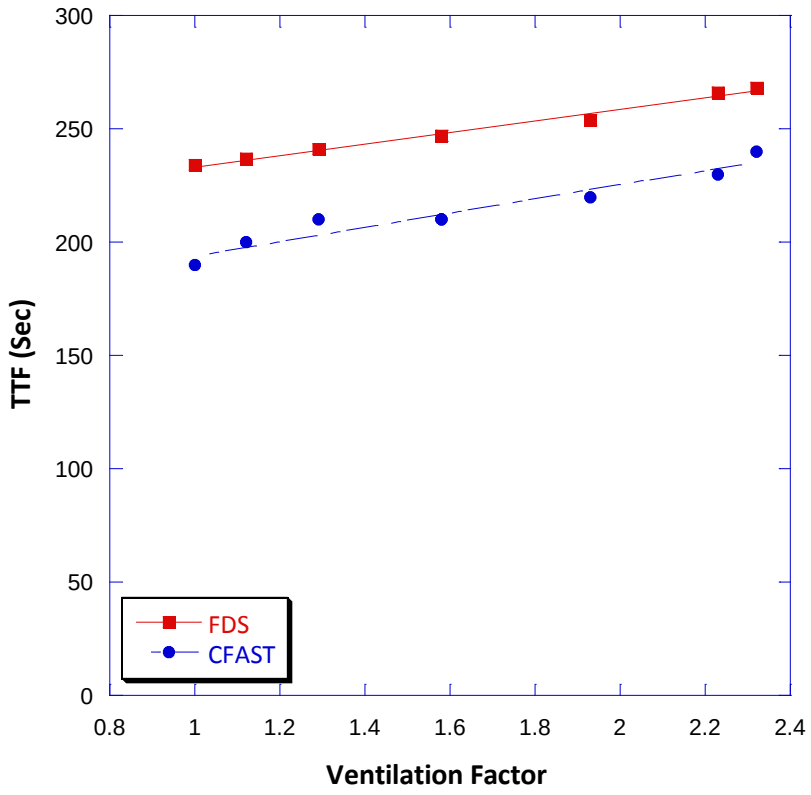

Figure 3.12: TTF Prediction of FDS and CFAST depending on Ventilation Factor

CHAPTER 4: Conclusions and Recommendations for Future Work

4.1 Summary and Conclusions

A pilot study of the development of flashover in enclosure fires was performed using the Fire Dynamics Simulator (FDS) platform. The capability of FDS in predicting the flashover in enclosure fires was investigated. The relation among the quantitative indicators for flashover was studied. Such quantifiable indicators include the heat flux to the floor, ceiling height temperature and upper layer temperature. were compared. FDS computation showed that 20kW/m^2 heat flux to the floor and 600 ℃ upper layer temperature can provide reliable flashover criteria independently of ceiling height, volume and ventilation conditions. It was shown that these two indicators also correspond with the onset of a sudden ramp of the heat release rate. Thus, 20kW/m^2 heat flux to the floor and 600 ℃ upper layer temperature can be regarded as a reliable flashover indicator according to FDS. However, a criteria based on 600℃ ceiling temperature underestimated TTF, especially for higher ceilings.

Compartment height was shown to influence the development of flashover. Taller ceilings increased time for flashover, even when the volume of the compartment was constant. The sensitivity of TTF to ceiling height for constant compartment volume revealed the importance of the hot gas layer on flashover. FDS computations were compared with those of zone models (CFAST and FASTLite) FDS demonstrated a higher sensitivity of TTF to volume and ceiling height than was one computed with two zone models.

The effect of the height of ventilation, size of ventilation and ventilation factor on the time required and the minimum heat release rate for the occurrence of flashover, and the maximum heat release rate after flashover was also investigated. FDS showed a the linear

relationship between ventilation factor and the maximum heat release rate and time to flashover, however, it failed to predict the pre-flashover heat release rate. That is, as the height of ventilation increased, the size of ventilation and the ventilation factor increased and the onset of flashover was delayed. This was because with higher ventilation factors, the air could more easily flow into and out of the compartment and the additional inflow increased the post-flashover heat release rate, and improved hot gas outflow, delaying TTF.

4.2 Possible Direction of Future Work

Further parametric studies based on the introduced factors would strengthen the validity of FDS predictions relating to flashvoer. Notably, the effects of ceiling geometry, such as the angle of the roof have not been studied much. Since it is widely accepted that the flashover is caused by radiation, it is worth investigating the effect of the angled-roof which potentially acts like a concave reflector and facilitate flashover. The validation and verification of the FDS code can be extended by comparing the results from FDS with experiments, thus, simple burn-cell experiments are necessary. The burn-cell should have a similar configuration to the computational setup as well as appropriate measurement apparatus. By putting thermocouples at the ceiling, the ceiling height temperature can be measured. In order to measure the upper layer temperature, a vertical series of thermocouples along the wall is necessary. Heat flux sensors will also be needed on the floor so that the heat flux to the floor can be measured. An IR camera will be needed to record the temperature field on the solid boundary, especially near ventilation openings.

Although it was proven here that FDS enhanced the capability to predict enclosure fires by performing a number of multi-grid calculations, the limit of computation cost still restricts an accurate numerical analysis. Practically, each computation performed by FDS in this thesis lasted on the order of twenty hours. Halving the resolution grid increases computation time by a factor of 16. More efficient computations can be performed by running FDS in parallel using MPI (Message Passing Interface) on a super-computing platform such as National Center for Supercomputing Applications (NCSA). In order to run FDS in parallel, the computational domain should be divided into multiple meshes so that the workload can be divided among the available processors.

REFERENCES

1. B. Karlsson and J. G. Quintiere, *Enclosure Fire Dynamics*, 1st Ed., CRC Press, New York, 2000.
2. W.D. Walton and P.H. Thomas, "Estimating temperature in compartment fires," in *The SFPE Handbook of Fire Protection ENGINEERING*, 2nd Ed., National Fire Protection Association, Quincy, 1995.
3. R. D. Peacock, P. A. Reneke, R. W. Bukowski and V. Babrauskas, "Defining Flashover for Fire Hazard Calculations," *Fire Safety Journal*: 331-345, 1998.
4. F.M. Liang, W.K. Chow and S.D. Liu, "Preliminary Studies on Flashover Mechanism in Compartment Fires," *Journal of Fire Sciences*: 87-112, 2002.
5. B. Hagglund, R. Jannson and R. Onnermark, "Fire development in residential rooms after ignition from nuclear explosions," *Forsvarets Forskningsanstalt*, Stockholm, 1974.
6. J.B. Fang, "Fire buildup in a room and the role of interior finish materials," *National Bureau of Standard, U.S.*, 1975.
7. E.K. Budnick and D.P. Klein, "Mobile home fire studies : summary and recommendations," *National Bureau of Standard, U.S.*, 79-1720, 1979.
8. E.K. Budnick, "Mobile home living room fire studies: the role of interior finish," *National Bureau of Standard, U.S.*, 78-1530, 1978.
9. D.P. Klein, "Characteristics of incidental fires in the living room of a mobile home," *National Bureau of Standard, U.S.*, 78-1522, 1978.
10. E.K. Budnick, D.P. Klein and R.J. O'Laughlin, "Mobile home bedroom fire studies: the role of interior finish," *National Bureau of Standard, U.S.*,78-1531,1978.
11. B.T. Lee and J.N. Breese, "Submarine compartment fire study – fire performance evaluation of hull insulation," *National Bureau of Standard, U.S.*, 78-1584, 1979.
12. V. Babrauskas, "Full-scale burning behavior of upholstered chairs," *National Bureau of Standard, U.S.*, TN 1103, 1979.
13. J.B. Fang and J.N. Breese, "Fire development in residential basement rooms," *National Bureau of Standard, U.S.*, 1980.

14. J.G. Quintiere, B.J. McCaffrey, "The burning of wood and plastic cribs in an enclosure: Vol. 1," *National Bureau of Standard, U.S.*, 80-2054, 1980.
15. P.H. Thomas, "Testing products and materials for their contribution to flashover in rooms," *Fire Material* 103-111, 1981.
16. W.J. Parker and B.T. Lee, "Fire build-up in reduced size enclosures," *Fire Safety Research*: 139-153, 1974.
17. E.E. Zukoski, T. Kubota and B. Cetegen, "Entrainment in fire plumes," *Fire Safety Journal*, Vol.3, 107-121, 1980.
18. G. Heskestad, "Fire Plumes," *SFPE Handbook of Fire Protection Engineering*, 2nd Ed. National Protection Association, Quincy, 1995.
19. B.J. McCaffrey, "Purely buoyant diffusion flames: Some experimental results," *National Bureau of Standard, U.S.*, 79-1910, 1979.
20. B.J. McCaffrey, J.G. Quintiere and M.F. Harkleroad, "Estimating room fire temperatures and the likelihood of flashover using fire test data correlations," *Fire Technology*, Vol 17, 98-119, 1981.
21. V. Babrauskas, "A closed-form approximation for post flashover compartment fire temperatures," *Fire Safety Journal*, 63-73, 1981.
22. P.H. Thomas, "Testing products and materials for their contribution to flashover in rooms," *Fire and Materials*, Vol. 5, 103-111, 1981.
23. K. Kawagoe, "Fire behavior in rooms," *Report of the building research institute, Japan*, No.27, 1958.
24. H.J Kim and D. G. Lilley, "Comparison of Criteria for Room Flashover," *Journal of Propulsion and Power*, Vol.3, 674-678, 2002.
25. R.D. Peacock, W.W. Jones, P.A. Reneke and G.P. Forney, *CFAST – Consolidated Model of Fire Growthand Smoke Transport (Version 6)*, National Institute of Standard and Technology, U.S., 2008
26. H.J Kim and D.G. Lilley, "Flashover: A Study of Parametric Effects on the Time to Reach Flashover Conditions," *Journal of Propulsion and Power*, Vol. 18, No. 3, 669–673, 2002.
27. NFPA, *Guide for smoke and heat venting*, NFPA 204M, National Fire Protection Association, Quincy, 1985.

28. H.J Kim and D. G. Lilley, "Flashover: A Study of Parameter Effects on Time to Reach Flashover Conditions," Journal of Propulsion and Power, Vol.18, 663-673, 2002.
29. K. McGrattan, R. McDermott, S. Hostikka and J. Floyd, *Fire Dynamics Simulator (Version 5) User's Guide*, National Institute of Standard and Technology, U.S., 2010.
30. K. McGrattan, S. Hostikka, J. Floyd, H. Baum, R. Rehm, W. Mell and R. McDermott, *Fire Dynamics Simulator (Version 5) - Technical Reference Guide*, National Institute of Standard and Technology, U.S., 2010.
31. D. Madrzykowski and W.D. Walton, "Cook County Administration Building Fire, 69 West Washington, Chicago, Illinois, October 17, 2003: Heat Release Rate Experiments and FDS Simulations," *NIST Special Publication SP-1021, National Institute Standards and Technology*, 2004.
32. NFPA, *The SFPE Handbook of Fire Protection ENGINEERING*, 5th Ed., National Fire Protection Association, Quincy, 1989.
33. S. Hostikka and K.B. McGrattan, "Large Eddy Simulation of Wood Combustion," *International Inter flam Conference 9th Proceedings*, Vol.1, 755-762, 2001.
34. T. Ma and J.G. Quintiere, "Numerical Simulation of Axi-symmetric Fire Plumes: Accuracy and Limitations," *MS Thesis*, University of Maryland, 2001.
35. P. Friday and F.W. Mowrer, "Comparison of FDS Model Predictions with FM/SNL Fire Test Data," *NIST GCR 01-810, National Institute of Standards and Technology, Gaithersburg*, 2001.
36. K.B. McGrattan, J.E. Floyd, G.P. Forney, H.R. Baum, and S. Hostikka, "Improved Radiation and Combustion Routines for a Large Eddy Simulation Fire Model," *Fire Safety Science, Proceedings of the Seventh International Symposium*, 827-838, 2002.
37. K.B. McGrattan, H.R. Baum, R.G. Rehm, "Large Eddy Simulations of Smoke Movement", *Fire Safety Journal*, V.30, 161-178, 1998.
38. M.L. Janssens and H.C. Tran, "Data Reduction of Room Tests for Zone Model Validation," *Journal of Fire Science*, 10, 528–555, 1992.
39. H.H Saber, A. Kashef, A. Bwalya, G. D. Lougheed and M.A. Sultan, *A numerical study on the effect of ventilation on fire development in a medium-sized residential room*, IRC-RR-241, Institute for Research in Construction, Canada, 2008.

APPENDIX A: FDS Code

```
&HEAD CHID='Burncell_V23', TITLE='IFSI Burn Cell Test'  /

&MESH IJK=48,64,48, XB=0.0,2.4,-0.8,2.4,0.0,2.4 /

&TIME TWFIN=500.0 /

&MISC SURF_DEFAULT='WALL' /

/Burner to initiate fire on chair/
&SURF ID          ='BURNER'
      HRRPUA      =3000.
      RAMP_Q      ='FIRE_RAMP'
      COLOR       ='RASPBERRY'/
&RAMP ID='FIRE_RAMP', T=0.00, F=0.00/
&RAMP ID='FIRE_RAMP', T=10.00, F=1.00/
&RAMP ID='FIRE_RAMP', T=140., F=1.00/
&RAMP ID='FIRE_RAMP', T=150., F=0.00/


/Chair combustible surface and material identification.  The upholsery is a
combination of fabric and foam./
/ As the chair burns the foam and fabric each release combustible fuel/

&SURF ID                     = 'UPHOLSTERY'
      COLOR                  = 'PURPLE'
      STRETCH_FACTOR         = 1.
      CELL_SIZE_FACTOR       = 0.5
      BURN_AWAY              = .TRUE.
      MATL_ID(1:2,1)         = 'FABRIC','FOAM'
      THICKNESS(1:2)         = 0.002,0.1/

&MATL ID                    = 'FABRIC'
      FYI                   = 'Properties completely fabricated'
      SPECIFIC_HEAT         = 1.0
      CONDUCTIVITY          = 0.1
      DENSITY               = 100.0
      N_REACTIONS           = 1
      NU_FUEL               = 1.
      REFERENCE_TEMPERATURE = 350.
      HEAT_OF_REACTION      = 3000.
      HEAT_OF_COMBUSTION    = 15000. /

&MATL ID                    = 'FOAM'
      FYI                   = 'Properties completely fabricated'
      SPECIFIC_HEAT         = 1.0
      CONDUCTIVITY          = 0.05
      DENSITY               = 40.0
      N_REACTIONS           = 1
      NU_FUEL               = 1.
      REFERENCE_TEMPERATURE = 350.
      HEAT_OF_REACTION      = 1500.
      HEAT_OF_COMBUSTION    = 30000. /
```

```
/Wall surface and material identification.  Wall material is assume not to
contribue additional fuel./
&SURF ID                      = 'WALL'
      RGB                     = 204,204,179
      MATL_ID(1,1)            = 'GYPSUM BOARD_MATL'
      MATL_MASS_FRACTION(1,1) = 1.00
      THICKNESS(1)            = 0.0130 /

&MATL ID                      = 'GYPSUM BOARD_MATL'
      SPECIFIC_HEAT           = 0.70
      CONDUCTIVITY            = 0.4800
      DENSITY                 = 450.00 /

/Carpet surface and material identification.  As carpet pyrolyzes it creates
a combustible fuel./
&SURF ID                      ='CARPET'
      RGB                     =153,204,255
      BURN_AWAY               = .TRUE.
      BACKING                 ='INSULATED'
      MATL_ID(1,1)            ='CARPET_MATL'
      MATL_MASS_FRACTION(1,1) =1.00
      THICKNESS(1)            =5.0000000E-003/

&MATL ID                      = 'CARPET_MATL'
      SPECIFIC_HEAT           = 1.00
      CONDUCTIVITY            = 0.1000
      DENSITY                 = 1290
      N_REACTIONS             = 1
      NU_FUEL                 = 1.00
      REFERENCE_TEMPERATURE   = 350.
      HEAT_OF_REACTION        = 3000.
      HEAT_OF_COMBUSTION      = 20000./

/Table surface and material identification.  When the wood burns it forms a
combustible fuel and char./

&SURF ID                        ='WOOD'
      RGB                       =128,51,26
      MATL_ID(1,1:3)            = 'CELLULOSE','WATER','LIGNIN'
      MATL_MASS_FRACTION(1,1:3) = 0.70,0.1,0.20
      THICKNESS                 = 0.0130   /

/Reaction 1: CELLULOSE is converted to "ACTIVE" solid fuel./

&MATL ID               = 'CELLULOSE'
      CONDUCTIVITY_RAMP = 'k_cell'
      SPECIFIC_HEAT    = 2.3
      DENSITY          = 400.
      N_REACTIONS      = 1
      A                = 2.8E19
      E                = 2.424E5
      HEAT_OF_REACTION = 0.
      NU_RESIDUE       = 1.0
      RESIDUE          = 'ACTIVE'/

/Reaction 2: "ACTIVE" solid is converted to CHAR and FUEL gases./
/Reaction 3: "ACTIVE" solid is converted FUEL gases./
```

```
&MATL ID                    = 'ACTIVE'
      EMISSIVITY            = 1.0
      CONDUCTIVITY_RAMP     = 'k_cell'
      SPECIFIC_HEAT         = 2.3
      DENSITY               = 400.
      N_REACTIONS           = 2
      A(1:2)                = 1.3E10,  3.23E14
      E(1:2)                = 1.505E5, 1.965E5
      HEAT_OF_REACTION(1:2) = 418.,    418.
      NU_RESIDUE(1:2)       = 0.35,    0.0
      NU_FUEL(1:2)          = 0.65,    1.0
      RESIDUE(1)            = 'CHAR' /

/The arguments (1:2) refer to the 2 REACTIONS./

/Conductivity ramps./

&RAMP ID='k_cell', T= 20., F=0.15 /
&RAMP ID='k_cell', T=500., F=0.29 /

&RAMP ID='k_char', T= 20., F=0.08 /
&RAMP ID='k_char', T=900., F=0.25 /

&RAMP ID='k_CASI', T= 20., F=0.06 /
&RAMP ID='k_CASI', T=400., F=0.25 /

/Water evaporation from original wood./

&MATL ID              = 'WATER'
      EMISSIVITY      = 1.0
      DENSITY         = 1000.
      CONDUCTIVITY    = 0.6
      SPECIFIC_HEAT   = 4.19
      N_REACTIONS     = 1
      A               = 1E20
      E               = 1.62E+05
      NU_WATER        = 1.0
      HEAT_OF_REACTION = 2260. /

&MATL ID              = 'LIGNIN'
      EMISSIVITY      = 1.0
      DENSITY         = 550.
      CONDUCTIVITY    = 0.1
      SPECIFIC_HEAT   = 1.1 /

&MATL ID                     ='CHAR'
      SPECIFIC_HEAT_RAMP     ='WOOD_CHAR_SPECIFIC_HEAT_RAMP'
      CONDUCTIVITY_RAMP      ='WOOD_CHAR_CONDUCTIVITY_RAMP'
      DENSITY                =120.00
      EMISSIVITY             =1.00/
&RAMP ID='WOOD_CHAR_SPECIFIC_HEAT_RAMP', T=20.00, F=0.68/
&RAMP ID='WOOD_CHAR_SPECIFIC_HEAT_RAMP', T=400.00, F=1.50/
&RAMP ID='WOOD_CHAR_SPECIFIC_HEAT_RAMP', T=900.00, F=1.80/
&RAMP ID='WOOD_CHAR_CONDUCTIVITY_RAMP', T=20.00, F=0.0770/
&RAMP ID='WOOD_CHAR_CONDUCTIVITY_RAMP', T=900.00, F=0.1600/
```

```
/Obstruction definitions for the geometry of the chair, first line is just
for the support structure and is assumed not to burn./
&OBST XB= 0.00, 0.80, 1.80, 2.20, 0.00, 0.40 /
&OBST XB= 0.00, 0.80, 1.80, 2.40, 0.40, 0.60, SURF_ID='UPHOLSTERY' / Chair,
left wall, seat cusion
&OBST XB= 0.00, 0.80, 1.60, 1.80, 0.00, 0.90, SURF_ID='UPHOLSTERY' / Chair,
left wall, right armrest
&OBST XB= 0.00, 0.80, 2.20, 2.40, 0.00, 0.90, SURF_ID='UPHOLSTERY' / Chair,
left wall, left armrest
&OBST XB= 0.00, 0.20, 1.80, 2.40, 0.00, 0.90, SURF_ID='UPHOLSTERY' / Chair,
left wall, back cushion

&VENT XB= 0.20, 0.30, 2.10, 2.20, 0.60, 0.60, SURF_ID='BURNER' / Ignition
source on chair

/Obstruction definitions for the geometry of the TV cart./
&OBST XB= 1.80, 2.40, 1.50, 2.40, 0.75, 0.80, SURF_ID='WOOD' / TV cart top
&OBST XB= 1.80, 1.90, 1.50, 1.60, 0.00, 0.80, SURF_ID='WOOD' / TV cart leg1
&OBST XB= 1.80, 1.90, 2.30, 2.40, 0.00, 0.80, SURF_ID='WOOD' / TV cart leg2
&OBST XB= 2.30, 2.40, 2.30, 2.40, 0.00, 0.80, SURF_ID='WOOD' / TV cart leg3
&OBST XB= 2.30, 2.40, 1.50, 1.60, 0.00, 0.80, SURF_ID='WOOD' / TV cart leg4
&OBST XB= 1.80, 1.85, 1.60, 2.30, 0.25, 0.75, SURF_ID='WOOD' / TV cart front
panel

/For ambient condition outside the room/
&VENT MB='YMIN',SURF_ID='OPEN' /
&VENT XB=0.0,0.0,-0.8,0.0,0.0,2.4,SURF_ID='OPEN' /
&VENT XB=0.0,2.4,-0.8,0.0,2.4,2.4,SURF_ID='OPEN' /
&VENT XB=2.4,2.4,-0.8,0.0,0.0,2.4,SURF_ID='OPEN' /

/Add front wall with window/
&OBST XB=0.0,2.4,0.0,0.01,0.0,2.4, SURF_ID='WALL'/
&HOLE XB=0.6,1.8,-0.01,0.02,0.6,1.8/

&VENT XB=0.00,2.4,0.00,2.4,0.00,0.00, SURF_ID='CARPET' /

/Outputs for visualization and quantification./
&BNDF QUANTITY='GAUGE_HEAT_FLUX' /
&BNDF QUANTITY='WALL_TEMPERATURE' /
&BNDF QUANTITY='BURNING_RATE' /

&SLCF PBX=1.20, QUANTITY='TEMPERATURE' /
&SLCF PBX=1.20, QUANTITY='V-VELOCITY'/
&SLCF PBX=1.20, QUANTITY='HRRPUV' / Heat Release Rate per Unit Volume

&SLCF PBX=0.80, QUANTITY='TEMPERATURE' /
&SLCF PBX=0.80, QUANTITY='V-VELOCITY'/
&SLCF PBX=0.80, QUANTITY='VELOCITY'/

&SLCF PBX=0.40, QUANTITY='TEMPERATURE' /
&SLCF PBX=0.40, QUANTITY='V-VELOCITY'/
&SLCF PBX=0.40, QUANTITY='HRRPUV' / Heat Release Rate per Unit Volume
&SLCF PBX=0.40, QUANTITY='MIXTURE_FRACTION' /
&SLCF PBX=0.40, QUANTITY='VOLUME FRACTION', SPEC_ID='oxygen'/

&SLCF PBY=2.10, QUANTITY='U-VELOCITY'/
```

```
&SLCF PBY=2.10, QUANTITY='TEMPERATURE'/
&SLCF PBY=2.10, QUANTITY='HRRPUV'/

/Output thermocouples and radiative heat flux of the both top and bottom
surface./

&DEVC ID = 'f1' ,XYZ=1.2,0.2,2.3, QUANTITY='TEMPERATURE' /
&DEVC ID = 'f2' ,XYZ=1.2,0.2,2.1, QUANTITY='TEMPERATURE' /
&DEVC ID = 'f3' ,XYZ=1.2,0.2,1.9, QUANTITY='TEMPERATURE' /
&DEVC ID = 'f4' ,XYZ=1.2,0.2,1.7, QUANTITY='TEMPERATURE' /
&DEVC ID = 'f5' ,XYZ=1.2,0.2,1.5, QUANTITY='TEMPERATURE' /
&DEVC ID = 'f6' ,XYZ=1.2,0.2,1.3, QUANTITY='TEMPERATURE' /
&DEVC ID = 'f7' ,XYZ=1.2,0.2,1.1, QUANTITY='TEMPERATURE' /
&DEVC ID = 'f8' ,XYZ=1.2,0.2,0.9, QUANTITY='TEMPERATURE' /
&DEVC ID = 'f9' ,XYZ=1.2,0.2,0.7, QUANTITY='TEMPERATURE' /
&DEVC ID = 'f10' ,XYZ=1.2,0.2,0.5, QUANTITY='TEMPERATURE' /
&DEVC ID = 'f11' ,XYZ=1.2,0.2,0.3, QUANTITY='TEMPERATURE' /
&DEVC ID = 'f12' ,XYZ=1.2,0.2,0.1, QUANTITY='TEMPERATURE' /

&DEVC ID = 'c1' ,XYZ=1.2,1.2,2.3, QUANTITY='TEMPERATURE' /
&DEVC ID = 'c2' ,XYZ=1.2,1.2,2.1, QUANTITY='TEMPERATURE' /
&DEVC ID = 'c3' ,XYZ=1.2,1.2,1.9, QUANTITY='TEMPERATURE' /
&DEVC ID = 'c4' ,XYZ=1.2,1.2,1.7, QUANTITY='TEMPERATURE' /
&DEVC ID = 'c5' ,XYZ=1.2,1.2,1.5, QUANTITY='TEMPERATURE' /
&DEVC ID = 'c6' ,XYZ=1.2,1.2,1.3, QUANTITY='TEMPERATURE' /
&DEVC ID = 'c7' ,XYZ=1.2,1.2,1.1, QUANTITY='TEMPERATURE' /
&DEVC ID = 'c8' ,XYZ=1.2,1.2,0.9, QUANTITY='TEMPERATURE' /
&DEVC ID = 'c9' ,XYZ=1.2,1.2,0.7, QUANTITY='TEMPERATURE' /
&DEVC ID = 'c10' ,XYZ=1.2,1.2,0.5, QUANTITY='TEMPERATURE' /
&DEVC ID = 'c11' ,XYZ=1.2,1.2,0.3, QUANTITY='TEMPERATURE' /
&DEVC ID = 'c12' ,XYZ=1.2,1.2,0.1, QUANTITY='TEMPERATURE' /

&DEVC ID = 'b1' ,XYZ=1.2,2.2,2.3, QUANTITY='TEMPERATURE' /
&DEVC ID = 'b2' ,XYZ=1.2,2.2,2.1, QUANTITY='TEMPERATURE' /
&DEVC ID = 'b3' ,XYZ=1.2,2.2,1.9, QUANTITY='TEMPERATURE' /
&DEVC ID = 'b4' ,XYZ=1.2,2.2,1.7, QUANTITY='TEMPERATURE' /
&DEVC ID = 'b5' ,XYZ=1.2,2.2,1.5, QUANTITY='TEMPERATURE' /
&DEVC ID = 'b6' ,XYZ=1.2,2.2,1.3, QUANTITY='TEMPERATURE' /
&DEVC ID = 'b7' ,XYZ=1.2,2.2,1.1, QUANTITY='TEMPERATURE' /
&DEVC ID = 'b8' ,XYZ=1.2,2.2,0.9, QUANTITY='TEMPERATURE' /
&DEVC ID = 'b9' ,XYZ=1.2,2.2,0.7, QUANTITY='TEMPERATURE' /
&DEVC ID = 'b10' ,XYZ=1.2,2.2,0.5, QUANTITY='TEMPERATURE' /
&DEVC ID = 'b11' ,XYZ=1.2,2.2,0.3, QUANTITY='TEMPERATURE' /
&DEVC ID = 'b12' ,XYZ=1.2,2.2,0.1, QUANTITY='TEMPERATURE' /


&DEVC ID = 'Heat flux_1.2' ,XYZ=1.2,1.2,0.0, QUANTITY='GAUGE HEAT FLUX', IOR
= 3. /
&DEVC ID = 'Heat flux_0.8' ,XYZ=1.2,0.8,0.0, QUANTITY='GAUGE HEAT FLUX' ,IOR
= 3./
&DEVC ID = 'Heat flux_0.4' ,XYZ=1.2,0.4,0.0, QUANTITY='GAUGE HEAT FLUX',IOR =
3./



&DEVC ID='layer height_c'
      QUANTITY='LAYER HEIGHT', XB = 1.2,1.2,1.2,1.2,0.0,2.4/
```

```
&DEVC ID='lower layer T_c', QUANTITY='LOWER TEMPERATURE'
      XB = 1.2,1.2,1.2,1.2,0.0,2.4/
&DEVC ID='upper layer T_c', QUANTITY='UPPER TEMPERATURE'
      XB = 1.2,1.2,1.2,1.2,0.0,2.4/

&DEVC ID='layer height_b'
      QUANTITY='LAYER HEIGHT', XB = 2.2,2.2,1.2,1.2,0.0,2.4/
&DEVC ID='lower layer T_b', QUANTITY='LOWER TEMPERATURE'
      XB = 2.2,2.2,1.2,1.2,0.0,2.4/
&DEVC ID='upper layer T_b', QUANTITY='UPPER TEMPERATURE'
      XB = 2.2,2.2,1.2,1.2,0.0,2.4/

&DEVC ID='layer height_f'
      QUANTITY='LAYER HEIGHT', XB = 0.2,0.2,1.2,1.2,0.0,2.4/
&DEVC ID='lower layer T_f', QUANTITY='LOWER TEMPERATURE'
      XB = 0.2,0.2,1.2,1.2,0.0,2.4/
&DEVC ID='upper layer T_f', QUANTITY='UPPER TEMPERATURE'
      XB = 0.2,0.2,1.2,1.2,0.0,2.4/



&TAIL /
```

APPENDIX B: CFAST Code

```
VERSN,6,CFAST Simulation
!!
!!Environmental Keywords
!!
TIMES,900,-50,0,10,10
EAMB,293.15,101300,0
TAMB,293.15,101300,0,40
CJET,WALLS
CHEMI,10,393.15
WIND,0,10,0.16
!!
!!Compartment keywords
!!
COMPA,Compartment 1,2.4,2.4,2,0,0,0,GYPSUM,OFF,GYPSUM
!!
!!vent keywords
!!
HVENT,1,2,1,1.2,1.8,0.6,1,0.6,0,1,1
!!
!!fire keywords
!!
OBJECT,New Fire,1,0.4,2,0,1,1,0,0,0,1
```